THE EFFECT OF FAST FLICKER ADAPTATION ON CONTRAST DISCRIMINATION

by

JAESEON SONG

(Under the Direction of James M. Brown)

ABSTRACT

Dynamic interactions between temporal and spatial frequency channels are crucial in visual processing. Recent studies have employed fast flicker adaptation (FFAd) to investigate the relationship between spatial and temporal vision, suggesting that FFAd primarily reduces sensitivity in the magnocellular (M) pathway at low spatial frequencies. Yet, the optimal conditions for FFAd and its neural mechanisms are not fully understood. We hypothesized that the M pathway's sensitivity to FFAd would be maximally affected by high temporal and low spatial frequencies, and that FFAd's impact on contrast discrimination would vary with the M pathway's response to different contrast levels. This study tested these hypotheses through three experiments, each designed to assess contrast discrimination following adaptation with flicker stimuli varying in (1) spatial contrasts, (2) spatial frequency components, and (3) temporal frequencies. Experiment 1 revealed that FFAd effects were most pronounced with high-contrast flicker. The findings emphasize the contrast response function derived from contrast discrimination tasks, offering a comprehensive view of function that enhances the insights from the contrast sensitivity function. Experiments 2 and 3 did not show significant effects of spatial or temporal frequencies, potentially due to flicker stimulus conditions. These results suggest FFAd's potential as a significant tool for advancing our understanding of spatiotemporal vision.

INDEX WORDS: fast flicker adaptation (FFAd), contrast discrimination, increment thresholds, Magnocellular, Parvocellular

THE EFFECT OF FAST FLICKER ADAPTATION ON CONTRAST DISCRIMINATION

by

JAESEON SONG

B.S., Chungbuk National University, 2013

M.S., Chungbuk National University, 2015

A Dissertation Submitted to the Graduate Faculty of The University of Georgia in Partial Fulfillment of the Requirements for the Degree

DOCTOR OF PHILOSOPHY

ATHENS, GEORGIA

2024

THE EFFECT OF FAST FLICKER ADAPTATION ON CONTRAST DISCRIMINATION

by

JAESEON SONG

Major Professor:	James M. Brown
Committee:	Billy R. Hammond Jr.
	Jennifer E. McDowell
	Bruno G. Breitmeyer

Electronic Version Approved:

Ron Walcott

Dean of the Graduate School

The University of Georgia

August 2024

ACKNOWLEDGEMENTS

I would like to express my deepest gratitude to all those who made it possible for me to complete this thesis. A special word of thanks goes to my advisor, James Brown, whose guidance, support, and encouragement were invaluable throughout this research. Jim, thank you for believing in me despite my struggles during the first few years. I now feel much more confident in my research due to your support.

I would also like to thank the other members of my dissertation committee, Billy Hammond, Jennifer McDowell, and Bruno Breitmeyer, for their helpful and warm commentary. I am particularly grateful for the assistance given by Dr. Breitmeyer at the University of Houston, whose insights and expertise added considerably to my understanding of visual pathways. Bruno, it has been an honor to collaborate with you. I admire your insights and pure excitement for research.

I also wish to acknowledge the support provided by the undergraduate students at UGA who patiently and diligently participated in my long experiments throughout the semester.

I am grateful to my family for their understanding and boundless love throughout my studies. Special thanks go to my mom, Jeong Mun Byun, my dad, Young Gil Song, and my sister, Imseon Song, for their unwavering encouragement and support over the years. Your belief in me kept me going. Lastly, I must express my heartfelt thanks to Tae Hyun Yoon, the love of my life, for always being there with wise counsel. You have made this journey, and my life, enjoyable and fulfilling. I could not have achieved this without you.

TABLE OF CONTENTS

Page

LIST OF TABLES

Page

LIST OF FIGURES

Page

The Effect of Flicker Adaptation on Contrast Discrimination

Introduction

Research suggests that the temporal and spatial channels of the visual system are intricately intertwined, with dynamic interactions across both dimensions. This notion is underscored by a multitude of studies spanning various fields, including visual masking (Breitmeyer et al., 1981; Breitmeyer & Ganz, 1976; Breitmeyer & Ganz, 1977; Breitmeyer & Williams, 1990; Hess & Snowden, 1992; Pokorny & Smith, 1997), figure-ground perception (Brown & Weisstein, 1988; Klymenko et al., 1989; Weisstein et al., 1992), and continuous flash suppression (CFS) (Han et al., 2018; Han et al., 2019; Han et al., 2016). For a more detailed review on history, see appendix.

Many of these investigations propose that the interaction between temporal and spatial channels is influenced by the relative contributions of the magnocellular (M) and parvocellular (P) pathways (see Figure 1). Historically, the M and P pathways have been delineated as the primary types of spatiotemporal channels. P neurons are typically more reactive to stimuli characterized by low temporal and high spatial frequencies. In contrast, M neurons exhibit increased responses to stimuli with high temporal and low spatial frequencies (Breitmeyer & Julesz, 1975; Breitmeyer & Ganz, 1977; Derrington & Lennie, 1984; Kaplan, 2004; Kaplan & Shapley, 1986; Kulikowski & Tolhurst, 1973; Legge, 1978; MacLeod, 1978; Merigan & Maunsell, 1993; Tolhurst & Movshon, 1975).

Visual masking has been a powerful tool to demonstrate complex spatiotemporal interactions in visual processing and shed light on 1) the time required to form a percept, 2) the

spatial range of influence between objects, and 3) visual processes that are beyond conscious awareness (For reviews, see Breitmeyer, 2007; Breitmeyer & Öğmen, 2006). Masking refers to the phenomenon where the visibility of a target object is significantly reduced by the presentation of another object, known as the mask. The effects on the visibility of the target are influenced by various spatial and temporal stimulus conditions of both the mask and the target.

In the temporal domain, forward masking occurs when the mask precedes the target, resulting in a reduction in the visibility of the briefly presented target. Conversely, backward masking happens when the target precedes the mask, yet the mask still reduces the visibility of the previously presented target. The magnitude of masking in both types is dependent on the stimulus onset asynchronies (SOAs), which is the time interval between the onset of the target and the mask.

Spatial factors, such as the size and the extent of spatial overlap between the target and mask patterns, introduce further complexities in the masking effects. Based on whether the target and the mask spatially overlap, visual masking can be categorized into two general types. In the first type, the elements of the patterned mask, composed of noise or a specific structure, spatially overlap with those of the target. The second type involves lateral masking, where the target and mask are spatially adjacent but do not overlap. For example, two adjacent rectangles or a disk surrounded by an annulus can produce lateral masking effects. These effects are observed in forms such as paracontrast (a type of forward masking where the mask temporally precedes the target) and metacontrast (a type of backward masking where the target temporally precedes the mask).

These masking effects have been attributed to interactions between M and P pathways. For instance, metacontrast has been linked to the transient response of the M pathway to the

mask, which is presented after the target. This response interferes with the P pathway's sustained response to the preceding target (Breitmeyer & Öğmen, 2006).

Additional evidence of spatiotemporal interactions in visual processing has emerged from psychophysical studies indicating that prolonged adaptation to temporal flicker (ranging from 10 s to 5 m) has an impact on human spatial vision (Arnold et al., 2016; Kaneko et al., 2015; Lee & Chong, 2021; Ye et al., 2021). These studies revealed that adapting to flicker at 8 Hz or higher resulted in a perceptual bias towards higher spatial frequencies (Arnold et al., 2016; Kaneko et al., 2015; Lee & Chong, 2021), or an increased sensitivity to the spatial frequency at which observers already showed peak sensitivity (Ye et al., 2021). The results suggest that fast temporal flicker adapts the M pathway, reducing sensitivity to low spatial frequencies. Arnold et al. named this phenomenon as fast flicker adaptation (FFAd).

FFAd holds potential as a method for exploring how human spatiotemporal vision works, possibly through the adaptation of the M pathway. The findings in humans are generally consistent with Solomon et al. (2004), which showed that prior adaptation to a high-contrast grating drifting at high temporal frequencies (≈ 11 Hz) led to a substantial and persistent reduction in the contrast sensitivity in lateral geniculate nucleus (LGN) M cells of macaque, but not in the P cells. Nonetheless, the optimal conditions for the adapting stimulus in FFAd are yet to be fully explored, and the results thus far reveal inconsistencies (see Table 1 for a comparative overview of stimulus conditions, measurements, and findings).

First, Arnold et al. (2016) and Lee and Chong (2021) observed adaptation to ultra-fast flicker rates, exceeding 60 Hz, induces a temporary shift in general spatial tuning toward higher spatial frequencies. Specifically, Arnold et al. reported a noticeable bias among observers towards higher spatial frequencies in face perception (Exp. 1) and improved text (three letters)

recognition (Exp. 3) following FFAd. It is established that face perception is primarily processed via the P pathway, specifically in the inferotemporal (IT) cortex (Afraz et al., 2006; Leopold et al., 2006; Sugase-Miyamoto et al., 2011; Vogels, 2022; Yamane et al., 1988). Arnold et al. interpreted the results to suggest that FFAd adapts the M pathway, diminishing M activity, which in turn results in reduced sensitivity to low spatial frequencies. Concurrently, the P pathway may either remain unaffected or possibly experience enhancement following FFAd, causing a shift in sensitivity towards higher spatial frequencies. However, the complexity inherent in face perception and text recognition, which involves a myriad of visual properties and intricate cognitive processing, complicates the interpretation of these results.

In their second experiment, they observed an enhancement in vernier acuity. However, this improvement may or may not support that FFAd adapts the M pathway, as some previous studies suggest that Vernier acuity is primarily mediated by the M pathway (Sun et al., 2008; Wehrhahn & Westheimer, 1990). For instance, Sun et al. (2008) discovered systematic inaccuracies in a vernier task due to contrast discrepancies with achromatic gratings; this issue was not observed with chromatic gratings. These results caution against hastily concluding that improved vernier acuity implies enhanced P- and decreased M-pathway activity.

In their final experiment, Arnold et al. (2016) measured contrast sensitivity. They observed that FFAd at 120 Hz specifically reduced sensitivity at low spatial frequencies, specifically 0.25 and 0.5 cycles per degree (cpd), in briefly presented static test stimuli. However, sensitivity remained consistent at higher spatial frequencies (2 cpd, 4 cpd, and 10 cpd). Although there was technically no change in sensitivity observed for moderate to high spatial frequencies, FFAd led to a decline in sensitivity for those below 2 cpd, tilting the balance of sensitivity in favor of higher spatial frequencies. Notably, adaptation to a low temporal

frequency of 0.8 Hz did not produce any FFAd effect.

More recently, Lee and Chong (2021) identified an enhancement in the precision of averaging orientations, sizes, and facial expressions (Exp. 1, 2, 3) following FFAd. Similar to the first two experiments by Arnold et al., these tasks either encompass a range of visual properties or involve intricate cognitive processing, or both. The multifaceted nature of these tasks complicates the task of identifying the spatiotemporal tuning of FFAd and obscures understanding of their origin.

Additionally, neither Arnold et al. (2016) nor Lee and Chong (2021) evaluated temporal frequencies ranging between 0.8 Hz and 60 Hz. In contrast, investigations by Kaneko et al. (2015) and Ye et al. (2021) probed these frequencies, investigating adapting flicker rates at 8 Hz and 12.5 Hz respectively, observing the most pronounced FFAd effect amongst various temporal frequencies. Specifically, Kaneko et al. revealed that flicker adaptation at 8 Hz increased perceived spatial frequencies of stationary test gratings, particularly at lower frequencies (0.25, 0.5, and 2 cpd). This effect was most pronounced at 8 Hz, with perceived spatial frequencies increasing by approximately 8%, in contrast to around 3% for other temporal frequencies (4 and 16 Hz). This enhancement diminished as spatial frequency increased, becoming negligible beyond 4 cpd.

The finding by Kaneko et al. (2015) of the FFAd effects at the low spatial frequencies of 0.25 to 2 cpd appears to align with Arnold et al. (2016). However, a direct comparison may be inappropriate given the distinctive characteristics of each study's test stimuli, as well as their adapting stimuli. In their study, Kaneko et al. varied the spatial frequencies of the test stimuli (Gabor patches) by adjusting the viewing distance, keeping the number of sinusoidal cycles constant. Similarly, Ye et al. (2021) used bandpass filtered digit stimuli. They kept the number of

sinusoidal cycles constant but changed the size of the digits to manipulate spatial frequency rather than modifying the viewing distance. Contrarily, Arnold et al. retained the size of their Gabor patches and varied the number of cycles. Such methodological divergences yield variations in the shapes of the CSF.

Research, including works by Mantiuk et al. (2022) and Watson and Ahumada (2005), has drawn comparisons between CSFs measured using stimuli of constant size (where the number of cycles varied) against those obtained using stimuli maintaining a constant number of cycles. As illustrated in Figure 2, a CSF using constant size stimuli—mirroring the methodology of Arnold et al. (2016)—exhibits a band-pass characteristic, peaking around 4 cpd (as illustrated on the left side of Figure 2). In contrast, a CSF obtained using a constant cycle count, similar to the approaches of Kaneko et al. (2015) and Ye et al. (2021), predominantly demonstrates a low-pass curve, peaking at 1 cpd (as represented on the right side of Figure 2). These nuanced differences in CSF profiles raise the possibility that the findings of Kaneko et al. and Ye et al. might have been influenced by the specific stimulus configuration chosen, suggesting potential variations if CSFs were assessed using constant-sized stimuli.

Moreover, Ye et al. (2021) observed FFAd effects solely at 12.5 Hz, with none at 60 Hz. This observation, along with Kaneko et al.'s (2015) finding of the most pronounced effect at 8 Hz, aligns with the established range of typical human temporal peak sensitivity, identified as being between 8−12 Hz (Cass & Alais, 2006; Kelly, 1966; Schwartz, 2004; Wooten et al., 2010). The optimal temporal frequencies for stimulating the M cells in the macaque LGN have been reported to be slightly higher, around 20 Hz (Derrington & Lennie, 1984; Hicks et al., 1983; Solomon et al., 2004). The lack of observed adaptation effect at 60 Hz by Ye et al. corresponds with the recognized high temporal frequency cutoff, often termed as critical flicker fusion

frequency, known to be between 50−60 Hz (de Lange Dzn, 1958; Kelly, 1961, 1972; Kulikowski & Tolhurst, 1973; Lloyd & Landis, 1960; Regan, 1968).

In a study on sensitivity to temporal flicker after flicker-adaptation, Shady et al. (2004) highlighted that the visual system can be adapted to uniform fields flickering at exceptionally high rates; however, peak modulation thresholds were notably prominent for adaptation frequencies ranging from 10 to 20 Hz. A significant reduction in test thresholds was observed when adaptation frequencies rose to 60 Hz, indicating that temporal frequencies of adapting flicker exceeding this threshold may not be as effective as those within the moderately fast flicker range. While these observations are exclusively examined in the temporal domain, they are congruent with the results acquired by Kaneko et al. (2015) and Ye et al. (2021).

Thus, several inconsistencies exist among prior studies regarding stimulus conditions and results that need resolution. Arnold et al. (2016), based on their final experiment, suggest that FFAd decreases sensitivity to lower spatial frequencies, specifically those less than 2 cpd. However, studies by Kaneko et al. (2015) and Ye et al. (2021) imply this effect could extend up to around 4 cpd, assuming test stimulus conditions analogous to those in Arnold et al.'s study were applied. These studies also reveal significant discrepancies in the temporal tunings of FFAd. While Arnold et al. and Lee and Chong found that ultra-fast flickers at and above 60 Hz are effective, Kaneko et al. and Ye et al. identified efficacy with moderately fast flickers around 10 Hz. Notably, Ye et al. did not observe an FFAd effect at 60 Hz.

To sum up, despite the variances in outcomes, a consensus seems to emerge, suggesting that FFAd typically induces relatively decreased sensitivity to lower spatial frequencies. However, a conflict exists regarding the reported temporal tuning of FFAd between the different study groups. The discrepancies in the temporal tuning of FFAd found by the studies brings into

question the results of Arnold et al. (2016) and Lee and Chong (2021), who reported FFAd effects at ultra-fast temporal frequencies (60 Hz and above) in their series of experiments. Theoretically, these frequencies might have a negligible effect. As previously mentioned, the M pathway is known to demonstrate a band-pass sensitivity that peaks at approximately 10 Hz and diminishes as frequencies move above or below this point (de Lange Dzn, 1958; Kelly, 1961, 1972; Kulikowski & Tolhurst, 1973; Lloyd & Landis, 1960; Regan, 1968). It stands to reason that if FFAd were occurring at temporal frequencies as high as 60 Hz and beyond, it would imply that we are essentially in a continuous state of adaptation when exposed to fluorescent lighting. Moreover, the frequencies employed by Arnold et al. and Lee and Chong exceed the typical human CFF threshold. Nevertheless, a consistent manifestation of the effect was observed in several experiments. What are the underlying reasons for this phenomenon?

The FFAd effect observed may be attributable to the unique spatial characteristics of dynamic noise patterns. Traditionally, research exploring flicker adaptation's impact on visual performance has primarily concentrated on the temporal domain, as seen in works like Shady et al., 2004. When focusing on temporal vision alone, employing a uniform pattern—as was done by Kaneko et al. (2015) and Ye et al. (2021)—seems suitable. Yet, when probing the effects of flicker adaptation on spatial vision, particularly with an aim to adapt the M pathway, stimuli exhibiting spatial features, such as dynamic noise patterns, could be more effective.

If FFAd effects stem from the adaptation of the M pathway, adopting conditions that preferentially stimulate this pathway might produce the most pronounced results. This pathway is known to prefer high temporal and low spatial frequencies and, as will be discussed in detail later, it typically demonstrates increased sensitivity to contrast, exhibiting higher contrast gain at low contrasts relative to the P pathway (Archer et al., 2021; Kaplan, 2004; Kaplan & Shapley,

1986). Hence, it stands to reason that a flickering stimulus with distinctive spatial properties, specifically low spatial frequency and spatial contrast information favored by the M pathway, would be more effective in adapting the M pathway compared to a uniformly flickering field.

Kaneko et al. (2015) and Ye et al. (2021) used spatially uniform patterns, with 100% luminance modulation, aligning with the approach taken in conventional temporal frequency research. Conversely, Lee and Chong (2021) used a dynamic noise pattern in the form of a grid (see the left side of Figure 3). This pattern displayed a mean luminance of 127 on a 0–255 luminance scale with a standard deviation of 50; each cell's side spanned 0.2°. The adaptation region covered by the dynamic noise pattern was 1.32 times larger than the test stimulus area. Although the specifics of their stimulus were not detailed in Arnold et al. (2016), it is assumed that they closely resembled those used by Lee and Chong, given that the latter adopted Arnold et al.'s methodology. In contrast to a spatially uniform pattern that has one luminance level, a random noise pattern can include various luminance levels, thereby introducing spatial components such as contrasts and spatial frequencies.

Also, retinal ganglion cells respond more strongly to spatially uniform fields than are LGN neurons whose responses might not be strong enough to detect changes induced by adaptation (Kaplan et al., 1987; Solomon et al., 2004). However, considering contrast discrimination is likely mainly mediated by post-retinal mechanisms (Song et al., 2024a; Song et al., 2024b), adaptation to high-contrast flicker can be very effective stimuli for both ganglion cells and LGN neurons (Solomon et al., 2004). These stimuli are also potent for inducing adaptation in cortical cells (Movshon & Lennie, 1979; Sclar et al., 1989).

Dynamic noise patterns are likely to be effective in adapting M cells in post-retinal processing due to three factors:

1. Various contrast levels are introduced in the patterns. Incorporating any level of contrast could potentially adapt the M pathway more effectively compared to zero contrast due to the M pathway's high sensitivity to contrasts.

2. The individual cells in each noise pattern are relatively large, hinting that the spatial frequencies of the patterns presented were likely biased more towards low than high spatial frequencies (see Figure 3).

3. The update rate of individual elements within dynamic noise patterns cannot be equated to the overall image flicker rate. The overall flicker rate exhibited in the studies by Arnold et al. (2016) and Lee and Chong (2021) might have been significantly slower than the intended ultra-fast rate, making it more resolvable.

The first factor potentially contributing to the M-biased nature of dynamic noise patterns is spatial contrast. Findings from studies involving recordings from the retina and LGN reveal that M neurons, in general, exhibit a high sensitivity to contrast compared to P neurons, with a notably higher contrast gain at lower contrasts, below 30% (Archer et al., 2021; Kaplan & Shapley, 1986; Lee et al., 1990; Purpura et al., 1988). BOLD responses measured by Tootell and Nasr (2017) from human V2 further substantiate this, illustrating a steeper increase in the contrast response function (CRF) of the M pathway at lower contrasts, relative to the P pathway (see Fig. 1 in Song et al., 2024a).

The dynamic noise patterns employed by Arnold et al. (2016) and Lee and Chong (2021) are presumed to primarily feature low to moderate spatial contrasts. This presumption stems from the randomness in the luminance of individual cells, which implies a low chance of presenting extreme luminance values across a pattern, along with the maintained mean luminance and the magnitude of the standard deviation. As such, it seems plausible that dynamic

noise patterns, compared to spatially uniform patterns with zero contrast, are more effective in activating and adapting the M pathway.

The second factor contributing to the M-biased nature of dynamic noise patterns is the incorporation of spatial frequencies, particularly the lower ones. These patterns cover a spectrum of spatial frequencies, but the power predominantly concentrates in the lower range. Figure 3 illustrates this, showing a noise pattern and its corresponding power spectrum. Viewed from a 60 cm distance, the pattern's power is mainly in low spatial frequencies below 2 cpd, which align with the M pathway's preference as outlined by numerous studies (Breitmeyer & Julesz, 1975; Breitmeyer & Ganz, 1977; Derrington & Lennie, 1984; Kaplan, 2004; Kaplan & Shapley, 1986; Keesey, 1972; Kelly, 1966, 1983, 1984; Kulikowski & Tolhurst, 1973; Legge, 1978; Lehky, 1985; Robson, 1966; Tolhurst & Movshon, 1975; van Nes et al., 1967). While high spatial frequencies are also included in dynamic noise patterns, there is an emphasis on the lower ones, potentially making them more effective, particularly in comparison to spatially uniform patterns, which lack spatial frequency information.

Finally, the update rate of individual elements within dynamic noise patterns is different from the overall image flicker rate. More precisely, there seems to have been a lack of control over the modulation depth (temporal contrast), as the mean luminance was not systematically varied in accordance with temporal frequency. We shall closely scrutinize these dynamic noise patterns. If both studies maintained the mean luminance at a pixel level—possibly 127, as outlined by Lee and Chong—the modulation depth tends toward zero. This is due to the consistent average luminance of the images, which does not vary over time. In their adapting stimuli, only the luminance levels of local cells were adjusted, leaving the mean luminance of the entire image unchanged.

Even at the local level, the dynamic noise patterns may not have achieved the intended frequency. In Figure 4, we provide an in-depth examination of the luminance modulation dynamics, differentiating between a 20-frame square wave and dynamic noise patterns modeled after Lee and Chong (2021). The average luminance is represented by a solid gray line. The luminance modulation of the square wave displays consistent peaks and troughs, delineated by a dashed gray line. Conversely, dynamic noise patterns exhibit irregular luminance modulations, represented by the solid black line. Specifically, as depicted in Figure 4a, even the smallest configuration, a single cell measuring 0.2° × 0.2°, reveals a pronounced difference in modulation compared to the square wave. Here, the square wave produces 10 cycles (comprising 10 peaks and 10 troughs) at full modulation, whereas the dynamic noise patterns' cells exhibit variability with only 5 to 6 cycles, characterized by irregularity and reduced modulation depths. This difference highlights the challenges in matching its frequency with that of the square wave. When analyzing larger configurations, such as the 36 cells (1.2° × 1.2°) example shown in Figure 4d —which still represents a relatively small portion of the visual field—the luminance curve begins to converge more closely to the mean luminance, posing even more challenges in matching its frequency with that of the square wave. Consequently, it is plausible to conclude that even at a local level, the dynamic noise patterns used in Arnold et al. (2016) and Lee and Chong encounter intrinsic difficulties in producing their target luminance modulation depths and temporal frequency across varied conditions, irrespective of the update rate, even at notably high rates.

Even if we assume a scenario where Arnold et al. (2016) and Lee and Chong (2021) did not maintain constant mean luminance for dynamic noise patterns, attaining the targeted overall image flicker rate would remain highly challenging, as meticulous control of modulation depth

and temporal frequency is required, beyond merely varying the rate of individual cells. Such a hypothesis finds its roots in studies on Continuous Flash Suppression (CFS) that share analogous stimulus characteristics with dynamic noise patterns.

In CFS, presenting incompatible images to each eye disrupts binocular fusion and leads to the suppression of one image, a phenomenon analogous to binocular rivalry. However, unlike binocular rivalry where one static image is presented continuously, CFS involves the presentation of updated images, incorporating the temporal aspect of vision. In this approach, one eye is exposed to a sequence of dynamic 'Mondrian' images, typically updated at a rate of 10 Hz, effectively suppressing a target image of low to moderate contrast in the other eye (Faivre & Koch, 2014; Kaunitz et al., 2014; Tsuchiya et al., 2006).

In a sequence of thorough investigations into CFS's temporal properties, a research group led by Han (Han et al., 2018; Han et al., 2019; Han et al., 2016) have used a unique approach to calculating temporal frequency when using a spatially complex flicker stimulus. Han and team hypothesized that the primary driver of CFS suppression comes from lower temporal frequencies than the commonly referenced 10 Hz. To validate this, they examined the temporal power spectrum for 70 grayscale Mondrian patterns. Similar to dynamic noise patterns, the luminance of each square of the patterns was randomly updated. They found a predominantly low-pass profile across varied temporal frequencies. For example, for the typical Mondrian flickering at 10 Hz, the stimulus energy at 10 Hz was minimal compared to 1 Hz, which had significantly more energy. They suggested that the likelihood of achieving the target flicker rate between consecutive updates is minimal. By managing to independently control both spatial and temporal dimensions, they found their stimuli with lower temporal frequencies (0.375, 0.75, 1.5, and 3 Hz) induced longer suppression duration than a static one and those with high temporal frequencies

(6.25, 12.5, and 25 Hz).

Therefore, even if each dynamic noise pattern possessed random mean luminance, in numerous locations within the patterns, cells likely experienced moderate, minimal, or no change, while cells in certain locations might have undergone significant shifts in modulation depths. Additionally, the probability of encountering extreme luminance values diminishes over prolonged periods, lengthening the modulation period and subsequently lowering the frequency, as depicted in Figure 4. This implies that the choice to update the luminance of individual cells within dynamic noise patterns, rather than adjusting the overall mean luminance to align with the intended temporal frequency, might have resulted in actual temporal frequencies significantly lower (slower) than the initially intended ultra-fast frequencies. This could be the reason the adapting stimuli employed by Arnold et al. (2016) and Lee and Chong (2021) triggered the FFAd effect.

The spatial characteristics inherent in dynamic noise patterns, exemplified by low contrasts and low spatial frequencies, may afford them an advantage over spatially uniform patterns. This advantage possibly stems from their alignment with the preferences of the M pathway. However, the stimuli employed by Arnold et al. (2016) and Lee and Chong (2021) do not appear to represent optimal conditions for testing the M-pathway hypotheses in FFAd, for several reasons. First, the luminance of individual cells, being determined randomly, hinders systematic comparison of FFAd effects across different contrast levels of the adapting stimulus. Second, while a grid structure with larger elements can better emphasize lower spatial frequencies compared to a standard white noise pattern with pixel-sized elements, the presence of cell boundaries prevents it from significantly diminishing the power at high frequencies (Figure 4). Third, merely updating the luminance of individual cells does not allow for

adjustments in modulation depths according to the targeted temporal frequency. This makes direct comparisons across different temporal frequencies infeasible. For accurate comparisons, each pattern's mean luminance should be systematically modified according to the intended temporal frequencies and modulation depths. Lastly, maintaining a constant grid pattern and only modifying cell luminance could result in afterimages that affect the perception of the test stimuli. If these unintended afterimages played a role in the observed effect, the enhanced spatial vision could be more due to spatial aftereffects on low spatial frequencies than to temporal flicker adaptation. These considerations emphasize the importance of a thorough examination of potential spatiotemporal variables in FFAd to discern their impact on spatial vision.

The Present Study

The aim of this study was to meticulously analyze the findings of prior research by scrutinizing the spatiotemporal variables—such as spatial contrast, spatial frequency, and temporal frequency—present in their adapting stimuli. The goal was to evaluate the efficacy of FFAd as a technique for adapting the M pathway and to discern its potential influence on spatial vision (Arnold et al., 2016; Kaneko et al., 2015; Lee & Chong, 2021; Ye et al., 2021). Additionally, we sought to pinpoint the optimal conditions for adapting stimuli in FFAd through precise control of the temporal and spatial aspects of the adapting stimuli. We hypothesized that for FFAd to effectively adapt the M pathway, the ideal conditions for adapting stimuli would likely encompass low contrasts, low spatial frequencies, and high temporal frequencies (around 10 Hz), reflecting the recognized preferences of the M pathway.

In everyday activities like reading, our visual perception interacts with stimuli that extend beyond mere light detection (absolute threshold). To fully examine changes in spatial vision, emphasizing contrast discrimination (difference threshold) alongside contrast detection (absolute

threshold) can be beneficial. The current study adopted this approach, evaluating the impact of FFAd on contrast increment thresholds, Δ*C*s.

Experiments 1 and 2 examined the effects of spatial contrast and spatial frequency of the adapting stimulus in FFAd, respectively, by analyzing shifts in Δ*C*s following FFAd. Experiment 3 delved into the temporal frequency tuning of FFAd. Collectively, our goal with these experiments was to underscore the potential of FFAd as a valuable tool for investigating the relationship between spatial and temporal vision, and for understanding the interplay between the M and P pathways.

Experiment 1: The Impact of Spatial Contrast of Adapting Flicker on Contrast Discrimination

Studies recording from the retina and LGN indicate that, generally, M neurons exhibit higher sensitivity to contrast compared to P neurons, with particularly higher contrast gain at lower contrasts (Archer et al., 2021; Kaplan & Shapley, 1986; Lee et al., 1990; Purpura et al., 1988). Specifically, the CRF for M neurons features a sharp initial increase with increased stimulus contrast, leveling off around 20–30% contrast (see Fig. 2 in Kaplan & Shapley, 1986). Conversely, P neurons present lower sensitivities to contrasts, displaying a more linear and gradual response to increasing stimulus contrast, resulting in similar contrast gains at higher contrasts to the M pathway. At low contrasts especially below 20%, Kaplan & Shapley (1986) observed that the contrast gain in LGN M cells was approximately ten times greater than that in LGN P cells.

Recently, Tootell and Nasr (2017) measured BOLD responses obtained from human V2 P-innervated thin stripes and V2 M-innervated thick stripes. Using their data, we formulated the CRFs for both the P and M pathways (see Fig. 1 in Song et al., 2024a). At human V2, both the P and M pathways show nonlinearity. Still, the CRF for the M pathway exhibited a sharp rise at low contrasts, plateauing around 10%. In contrast, the CRF for the P pathway in V2 displayed a much more gradual incline.

Studies involving the human cortex, as well as the animal retina and LGN, emphasize the significantly steeper CRF of the M pathway at low contrasts in comparison to the P pathway. At a low contrast of 10%, the M pathway demonstrates pronounced responsiveness, while the P

pathway's response is comparatively muted. As a result, a 10% contrast in adapting stimuli might be sufficient to effectively adapt the M pathway.

The objectives of Experiment 1 were fourfold:

1. FFAd Effect: The first objective was to determine if fast flicker with 10% and 50% contrasts (10C-F and 50C-F conditions) and without contrast (0C-F condition, uniform pattern) can adapt the M pathway, relative to a static, luminance adaptation condition (0C-S condition, baseline). We hypothesized that Δ*C*s would be higher for flicker conditions (0C-F, 10C-F, and 50C-F) than for the static luminance adaptation (0C-S). Given the M pathway's predominant role in processing low spatial frequencies, we expected that FFAd would lead to a decline in contrast discrimination, indicated by increased Δ*C*s, specifically in the low spatial frequency (0.5 cpd) test condition. Conversely, we anticipated that contrast discrimination would remain unaffected in the high spatial frequency condition (5 cpd), as it is primarily mediated by the P pathway.

2. Effect of Spatial Contrast Information of Adapting Flicker: Next, we sought to examine whether adapting flicker with contrast can yield higher adaptation effects on contrast discrimination than a uniform pattern, at low spatial frequencies. This approach contrasts with the exclusive use of temporal modulation (temporal contrast) of a uniform pattern without spatial contrasts, as used in Ye et al. (2021). Technically, Kaneko et al. did not employ a completely uniform pattern; rather, they introduced some degree of contrast by using an adapting stimulus where either the top or bottom half was subject to flickering. Observers were instructed to maintain fixation at the center, which likely resulted in a perceptible contrast between the two flickering and non-flickering halves.

Given the known higher sensitivity of the M pathway to low contrast compared to the P pathway, we theorized that adapting flicker conditions with contrast, both 50% (50C-F) and 10%

(10C-F) would induce stronger adaptation effects on contrast discrimination at the low spatial frequencies, mediated by the M pathway, than a flicker condition at 0% contrast (0C-F), which only involves temporal modulation of a uniform pattern. Consequently, we anticipated higher Δ*C*s in the 50C-F and 10C-F conditions compared to the 0C-F condition, specifically at 0.5 cpd, rather than 5 cpd.

3. Influence of High-Contrast Adapting Flicker: The third objective was to assess whether the effects of FFAd on Δ*C*s vary depending on the contrast level of the adapting flicker, with a particular focus on whether high-contrast adapting flicker produces a greater adaptation effect. Solomon et al. (2004) observed that adaptation to a fast-moving, high-contrast grating resulted in reduced contrast sensitivity in the M neurons of the macaque LGN. Considering that motion and flicker might elicit different effects and that physiological responses in macaque cells may not directly correlate with human contrast discrimination, we aimed to investigate whether a high-contrast adapting flicker would result in a more pronounced adaptation effect compared to a low-contrast flicker, specifically at low spatial frequencies. Therefore, we hypothesized that an adapting flicker with the highest contrast of 50% (50C-F) would induce the highest Δ*C*s at 0.5 cpd, rather than at 5 cpd, compared to all other conditions (0C-S, 0C-F, and 10C-F).

Moreover, existing retinal, LGN, (Archer et al., 2021; Kaplan & Shapley, 1986; Lee et al., 1990; Purpura et al., 1988) and cortical data (Tootell & Nasr, 2017) suggest that the M pathway's contrast gain is exceptionally high at low contrasts (≈10% or less). This implies that the high-contrast adapting flicker may effectively reduce contrast discrimination performance of the M pathway (increase Δ*C*s at 0.5 cpd), particularly at low test contrasts. Alternatively, it might generally affect contrast discrimination across all test contrast levels.

4. Contrast discrimination as a complement to contrast detection: Lastly, the contrast

sensitivity function (CSF), measured by detection thresholds, has traditionally been emphasized in vision science research, and its foundational principles and findings are well-covered by Mantiuk et al. (2022). However, the contrast response function (CRF), measured by discrimination thresholds, may provide a more comprehensive assessment of FFAd effects, offering deeper insights compared to solely focusing on contrast detection thresholds. We hypothesized that the impact of FFAd on contrast discrimination, as indicated by increment thresholds (Δ*C*s), would parallel the effects observed in contrast detection thresholds (Δ*C*s at 0% pedestal contrast of test Gabor patches, where there is no baseline contrast for comparison). This approach aims to provide a more comprehensive assessment of the changes resulting from adaptation.

To explore these hypotheses, we assessed the impacts of adapting flickers with 0% (both static and flickering), 10%, and 50% contrasts on ΔCs as a function of pedestal test contrasts (0%, 10%, 30%, and 50%) for 0.5 and 5 cpd test stimuli. For the adapting flicker, we employed a configuration consisting of a smaller circle within a larger circle (Figure 5). The Michelson contrast was calculated using the luminance values of the smaller circle (maximum) and the larger circle (minimum). The background luminance was set at the mean of the luminance values of both circles and was modulated following a sine-wave pattern. In the 0% contrast condition, the inner and outer circles and the background had the same luminance, resulting in a uniform pattern adaptation condition akin to those used by Kaneko et al. (2015) and Ye et al. (2021).

Anticipating that the combination of lower spatial frequencies with higher temporal frequencies would create optimal conditions for the adapting flicker, we Gaussian-windowed both circles to eliminate high spatial frequencies and set the temporal frequency at 10.6 Hz. For the test Gabor patches (sinusoidal gratings), to prevent the potential confounding factor of size,

we varied the spatial frequency by keeping the size of the test stimuli constant and adjusting the number of cycles.

Method

Participants. The study involved nine participants from the University of Georgia, including undergraduate and graduate students, as well as a professor. Of these participants, five were female and four were male, with all individuals aged 18 years or older. Each individual either possessed normal visual acuity or had their vision corrected to normal standards using glasses or contact lenses. Prior to participation, all individuals provided informed consent in alignment with the ethical guidelines set by the University of Georgia's Institutional Review Board.

Power Analysis. Sample size determination for each experiment was conducted using the “Bias and Uncertainty Corrected Sample Size” (BUCSS) R package (Anderson et al., 2017, Version 1.2.1). Contrary to traditional approaches, which necessitate estimated effect sizes, BUCSS uses observed *t* or *F* values and sample size to recommend sample sizes for planned studies. *F* values from notable main effects reported in prior research were employed as inputs for the BUCSS "ss.power.wa.general()" function.

In conducting our power analysis, our primary reference was the finding from Kaneko et al. (2015), because the studies by Arnold et al. (2016) and Lee and Chong (2021) appeared to inaccurately evaluate the temporal frequencies they used, likely because of imprecise flicker depth modulation. Additionally, the procedure used by Ye et al. (2021) entailed consistently measuring the baseline condition before the experimental condition, which introduces the possibility of practice effects influencing the results.

In determining our sample size, we therefore utilized the findings of Kaneko et al. Drawing from their study, we used the same *F* values tailored to our repeated measures design,

encompassing four contrast levels for adapting stimuli, four contrast levels for test stimuli, and two spatial frequencies for test stimuli. For the analysis parameters, we set “alpha.prior” to 0.05, “alpha.planned” also to 0.05, “assurance” to 0.8, and targeted a “power” of 0.8. The results suggested a need for six participants when considering spatial frequencies, four participants when looking at contrasts for either adapting or test stimuli, and two for the three-way interaction effect. To ensure a robust study design, even though the analysis called for six participants, we decided to include nine participants in total.

Apparatus and stimuli. Test stimuli were created using PsychoPy v.2021.2.3 (Peirce, 2007) and were presented on a calibrated Samsung SyncMaster 1100DF monitor. The monitor operated at an 85 Hz refresh rate and its screen resolution was 1024 × 768. Calibration was achieved with the assistance of a Photo Research PR-650 Spectrophotometer. The testing room was set up so that the monitor served as the sole source of light. Participants viewed the display binocularly from a fixed distance of 58 cm using a chin rest equipped with a forehead support to maintain a stable head position.

To establish varying contrast levels for our adapting stimuli, we used a configuration in which a smaller circle with a diameter of 3° was contained within a larger circle measuring 8.2° in diameter. Our first step was determining the mean luminance values to match a sine-wave form, modulating at 50%. As seen in Figure 5a, using the Michelson contrast formula, $C = (L_{max} - L_{min})/(L_{max} + L_{min})$, and taking the mean luminance values as our reference, we computed the corresponding luminance values for the inner (L_{max}) and outer (L_{min}) circles. All these values were modulated in alignment with a sine-wave pattern. The overall mean luminance across all images was 30 cd/m^2.

We established four contrast conditions for the adapting stimuli (Figure 5b): 0C-S (0%

Contrast, Static), 0C-F (0% Contrast, Flickering), 10C-F (10% Contrast, Flickering), and 50C-F (50% Contrast, Flickering). The 0C-S baseline condition was a static uniform gray field devoid of contrast or temporal changes. Differing from this, the 0C-F condition maintained the same gray field but introduced a flicker with 50% modulation, thereby adding a temporal dimension without altering contrast, yielding a condition of pure temporal modulation.

For conditions involving contrast, namely 10C-F and 50C-F, stimuli consisted of two Gaussian-windowed ($\sigma = 0.06°$) circles that minimized high spatial frequencies. These patterns concentrated their spatial frequency energy predominantly below 2 cpd. The temporal frequency for the three flickering conditions was consistently set at 10.6 Hz. For the adaptation period, we chose a duration of 30 seconds, drawing on findings from prior studies on motion aftereffects (Bartlett et al., 2018; Huk et al., 2001; Murd & Bachmann, 2011; Nishida & Ashida, 2000; van de Grind et al., 2004). For a detailed description of the timing control mechanisms and evaluation procedures employed across all experiments, refer to the method section in Experiment 2.

For the test stimuli, Gabor patches were used. Each patch featured a sinusoidal grating, covering 4° of visual angle, enveloped within a Gaussian window ($\sigma = 0.1°$). Although the entire grating extended to 4°, only a portion with a diameter less than 3° was distinctly visible. Consequently, each patch's center was offset by 1.5° from the center of the display, positioned either to the left or the right, ensuring no visible overlap between patches in any condition. The pedestal contrasts of the Gabor patches were 0%, 10%, 30%, and 50%, based on the Michelson contrast. The spatial frequencies tested were 0.5 and 5 cpd. In varying the spatial frequency, we kept the size of the test stimuli constant but altered the number of cycles within them. To aid in fixation, two vertical lines, each measuring 1°, were positioned on the display — one above and

the other below the center of the test stimulus.

Design and procedure. The experiment incorporated 32 stimulus conditions per participant, derived from a combination of: four adapting stimuli contrasts, four test pedestal contrasts, and two test spatial frequencies. Each participant underwent three sessions (repetitions), with each session consisting of four blocks. These blocks corresponded to the four contrast conditions of the adapting stimuli. Within each block, there were eight conditions, accounting for the four test pedestal contrast levels and the two test spatial frequencies. The order of sessions, blocks within each session, and conditions within each block were all determined pseudo-randomly.

Before the experiment began, participants underwent a 15-m period of dark adaptation. As represented in Figure 8, each block began with a 30-s flicker adaptation. This was followed by trials with a 3-s flicker adaptation top-up. The first trial of subsequent conditions within a block had a 15-s flicker adaptation. Following the adaptation phase, a one-second inter-stimulus interval (ISI) ensued, within which an auditory cue was sounded at 400 milliseconds to signal the imminent presentation of the subsequent test stimulus. The test display appeared for 106 ms, after which participants identified whether the left or right Gabor patch had a higher contrast using a two-alternative forced choice (2AFC) task. Responses influenced the contrast of the subsequent pedestal Gabor patch, which was adjusted via the adaptive QUEST procedure (Watson & Pelli, 1983). The parameters were set at: 75% for threshold criterion, 0.01 for delta, and 0.5 for gamma. Each condition concluded when the 95% confidence width reached 0.17.

After each block, a 2-minute break was given to help prevent adaptation carryover effects. Before the main experiment began, participants underwent practice trials to familiarize themselves with the contrast discrimination task. During this practice session, they were presented with 10 examples: two examples of test spatial frequencies that were easily

distinguishable (though not used in the main experiment) and actual samples from the eight conditions (4 test pedestal contrasts × 2 test spatial frequencies). Following this, they carried out 10 to 15 trials in one condition that was pseudo-randomly chosen, with a brief 4-s initial adaptation and 2-s top-up adaptations.

Analysis. Each participant was exposed to 32 unique conditions, derived from the combination of two test spatial frequencies (0.5 cpd and 5 cpd), four test pedestal contrasts (0%, 10%, 30%, 50%), and four contrast conditions of adapting flicker (0C-S, 0C-F, 10C-F, 50C-F). For each unique condition, the participant's Δ*C* for each condition was measured three times. We averaged the three measurements of Δ*C*s for each condition for every participant, which were then used for subsequent statistical analyses.

We conducted a 4 (adapting flicker contrast) × 2 (test spatial frequency) × 4 (test pedestal contrast) repeated measures ANOVA on these averaged Δ*C* values to assess the main effects and interactions of our independent variables on the Δ*C*. When necessary, Benjamini-Hochberg post-hoc tests were conducted.

Results

A three-way repeated measures ANOVA conducted on the increment threshold (Δ*C*) data indicated significant main effects of adapting flicker contrast, $F(3, 24) = 5.64$, $p = .005$, $\eta^2 = .044$, and test pedestal contrast, $F(3, 24) = 59.5$, $p < .001$, $\eta^2 = .624$. Additionally, significant two-way interactions were observed between adapting flicker contrast and test spatial frequency, $F(3, 24) = 10.24$, $p < .001$, $\eta^2 = .052$, and between test spatial frequency and test pedestal contrast, $F(3, 24) = 3.52$, $p = .03$, $\eta^2 = .056$. Mauchly's test indicated that there was no violation of sphericity.

To further analyze these significant interactions, simple main effects were computed. As

can be seen in Figure 6a, the analyses of simple main effects revealed that the contrast of adapting flicker significantly affected Δ*C*s only at 0.5 cpd at 0% [$F(3, 24) = 12.6$, $p < .001$, $\eta^2 = .374$], 10% [$F(3, 24) = 3.48$, $p = .032$, $\eta^2 = .120$], and 30% [$F(3, 24) = 5.66$, $p = .004$, $\eta^2 = .313$] of test Gabor contrast. The pedestal contrast of the test Gabor patches consistently showed significant simple main effects across all conditions of test spatial frequencies and adapting flicker contrasts (all $p < .001$).

Following the observation of significant simple main effects for adapting flicker contrast, pairwise comparisons (one-tailed) with Benjamini-Hochberg corrections to adjust for multiple comparisons were performed. These analyses supported our first hypothesis that FFAd conditions (50C-F, 10C-F, and 0C-F) would yield higher Δ*C*s relative to the static, luminance adaptation condition (0C-S), particularly at the low spatial frequency of 0.5 cpd under contrast detection task (0% test pedestal contrast). Specifically, at 0.5 cpd and 0% test pedestal contrast, fast flicker conditions—50C-F ($p < .001$), 10C-F ($p < .001$), and 0C-F ($p = .025$)—resulted in higher Δ*C*s compared to 0C-S condition. However, although the 0C-F condition without spatial contrast tended to yield higher Δ*C*s, these differences were not statistically significant compared to the baseline 0C-S condition at other contrast levels of the test Gabor patches.

Our second and third hypotheses were also confirmed. Adapting flicker with contrast generally yielded higher adaptation effects on contrast discrimination than a uniform pattern, especially at low spatial frequencies. Moreover, the high-contrast adapting flicker condition (50C-F) produced the strongest adaptation effects across the most test conditions, at lower test pedestal contrasts. Specifically, at 0.5 cpd and 0% test pedestal contrast, the 50C-F condition resulted in higher Δ*C*s compared to the 0C-S ($p < .001$), 0C-F ($p = .025$), and 10C-F ($p = .033$) conditions. At the same test spatial frequency but with a 10% test pedestal contrast, the 50C-F (*p*

= .024) and 10C-F ($p < .001$) conditions showed higher Δ*C*s than the 0C-S condition. At 30% test pedestal contrast, the 50C-F condition exhibited significantly increased Δ*C*s relative to all other adapting conditions: 0C-S ($p = .020$), 0C-F ($p = .007$), and 10C-F ($p = .031$). As seen in Figure 6a, although the 50C-F condition also tended to increase ΔCs at 50% test pedestal contrast, these differences were not statistically significant.

To evaluate our fourth prediction, we analyzed the correlations between the effects of various flicker adaptation conditions on Δ*C*s (the CRF curves under different adapting conditions) across test pedestal contrasts at 0.5 cpd and 5 cpd test spatial frequencies. Pearson's correlation coefficients were computed to create a correlation matrix, as shown in Figure 6b. Positive correlations are marked in lighter shades, negative in darker shades, with color intensity indicating correlation strength from high (white for strong positive correlations) to low (black for strong negative correlations), with gray representing zero correlation. As expected, the matrix reveals strong positive correlations (lighter shades) at 0.5 cpd (left panel in Figure 6b). The sequence of ΔCs (with 50C-F highest, followed by 10C-F, 0C-F, and 0C-S the lowest) for the contrast detection task at 0% test pedestal contrast, which measures contrast sensitivity is consistently maintained across different test pedestal contrasts in the contrast discrimination task that measures contrast response.

However, this order does not hold at the higher spatial frequency of 5 cpd (right panel in Figure 6b), with coefficients ranging from -0.95 to 0.97, highlighting varied interactions at this higher frequency. As illustrated in Figure 6a, all CRF curves for adapting flicker conditions—except for the static 0C-S condition—show dips at the 10% test pedestal contrast. Specifically, two-tailed pairwise comparisons revealed that at 5 cpd under the 0C-F adapting flicker condition, the 10% test pedestal contrast resulted in lower Δ*C*s compared to other test pedestal contrasts:

0% (p = .048), 30% (p < .001), and 50% (p < .001). Similarly, under the 10C-F condition at the same test spatial frequency, 10% test pedestal contrast yielded lower ΔCs compared to 0% (p = .049), 30% (p < .001), and 50% (p < .001). Under the 50C-F condition, 10% test pedestal contrast also resulted in lower ΔCs compared to the 30% test pedestal contrast (p = .004).

Discussion

Our findings indicate that FFAd reduced contrast sensitivity (detection thresholds at 0% test pedestal contrast) at a low spatial frequency test condition of 0.5 cpd, irrespective of whether the adapting flicker contained contrast (50C-F, 10C-F) or not (0C-F), compared to the static, luminance adaptation condition (0C-S). This effect was not observed at the higher spatial frequency of 5 cpd. This pattern suggests that FFAd selectively adapts M pathway activity, which is sensitive to stimuli with high temporal and low spatial frequencies, thus supporting our first hypothesis and previous findings (Arnold et al., 2016; Kaneko et al., 2015; Ye et al., 2021). Although the 0C-F condition, which lacks spatial contrast, tended to result in higher ΔCs compared to the 0C-S condition, these differences were not statistically significant at higher test pedestal contrasts (under contrast discrimination tasks). This finding suggests that flicker adaptation with a uniform pattern predominantly influences M pathway-mediated contrast sensitivity (detection thresholds) rather than M pathway-mediated contrast responses (discrimination thresholds). A more in-depth discussion of this will be provided in the general discussion section.

When adapting flicker includes high contrast, FFAd significantly increases ΔCs for both detection thresholds at 0% test pedestal contrast and discrimination thresholds at other test pedestal contrasts at the low spatial frequency (0.5 cpd). This indicates a reduction in both M pathway-mediated contrast sensitivity and contrast responses. This finding supports the results

observed in the macaque study by Solomon et al. (2004) and our third hypothesis. The highest adaptation effect of 50C-F condition is maintained across all test pedestal contrasts. At the highest test pedestal contrast of 50%, while the difference was not statistically significant, this condition still tended to yield the highest Δ*C*s.

Including contrast in the adapting flicker was more effective than using a uniform pattern flicker, consistent with our second hypothesis and the findings of Arnold et al. (2016). For instance, at a 10% test pedestal contrast, adapting flicker conditions that included contrast (10C-F and 50C-F) led to significantly higher Δ*C*s compared to the uniform static (0C-S) condition. In contrast, the condition with a uniform pattern featuring only temporal modulation (0C-F) did not produce significantly higher Δ*C*s compared to the 0C-S condition. This observation suggests while low-contrast adapting flicker may not be as effective as high-contrast adapting flicker, it is still more effective in diminishing the M-mediated contrast discrimination than uniform pattern flicker. This emphasizes that contrast of adapting flicker can be an important factor in adapting M pathway processes.

The differences in ΔCs at 0.5 cpd between the adapting flicker conditions and the static condition were statistically significant at relatively low test pedestal contrasts (0% to 30%), but not at 50%. This could be attributed to the possibility that fast flicker adaptation (FFAd) particularly reduces the M pathway's contrast gain. Alternatively, the findings might be influenced by the relatively small sample size; although our sample size exceeded the number suggested by our power analysis, which was based on prior research, the results from the ANOVA could still be sensitive to sample size effects.

In line with our fourth hypothesis, the relationships among the adapting flicker conditions for the contrast detection task (0% test pedestal contrast) were consistently maintained for the

contrast discrimination task across different test pedestal contrasts at 0.5 cpd. However, this consistency was not observed at the higher spatial frequency of 5 cpd. This finding suggests that measuring contrast discrimination alongside contrast detection following FFAd can provide a more comprehensive approach to examining M pathway processing. Moreover, individuals with impaired M pathway function may exhibit different response curves across various test pedestal contrasts, further highlighting the value of integrating these measures to understand visual adaptation processing differences.

Arnold et al. (2016) observed decreased contrast sensitivity at lower spatial frequencies (0.25 and 0.5 cpd) but did not find any increase in contrast sensitivity at higher spatial frequencies. In our study, we noted similar patterns in contrast sensitivity: a reduction at the lower spatial frequency of 0.5 cpd without an increase at the higher spatial frequency of 5 cpd. However, our findings in contrast discrimination at 5 cpd revealed notable results. Specifically, at the 10% test pedestal contrast, compared to other test pedestal contrasts, we recorded decreased ΔCs (indicating increased contrast response) under all flicker adapting conditions, except the static condition (as shown in the right panel of Figure 6a). While we treat this new finding with caution, it suggests that only contrast discrimination, not contrast sensitivity, may detect this difference. It is important to note that results from other studies (Kaneko et al., 2015; Lee & Chong, 2021; Ye et al., 2021) are not directly comparable due to variations in measurement tasks and stimuli used. The observed difference at the 10% test pedestal contrast may be explained by antagonistic interactions between the M and P pathways, where decreased activity in the M pathway could lead to relatively increased activity in the P pathway. For further theoretical insight on the antagonistic interactions between the M and P pathways, see reviews by Brown (2018) and Weisstein et al. (1992). Based on this theory, our results could be

interpreted to suggest that flicker adaptation enhances contrast discrimination mediated by the P pathway through specific adaptation of the M pathway's contrast gain at low contrasts. Also, considering that the differences in increased ΔCs (indicating decreased contrast sensitivity and response) at 0.5 cpd between the adapting flicker conditions and the static condition were more pronounced at relatively low test pedestal contrasts (0% to 30%), it appears that the M pathway's contrast gain may be more significantly affected by FFAd. This may explain why we observed increased contrast response at the 10% contrast in the 5 cpd condition.

Experiment 2: The Impact of Spatial Frequency in Adapting Flicker on Contrast Discrimination

In Experiment 2, we sought to explore an additional factor that might influence the FFAd effect on increased sensitivity to higher spatial frequencies: the spatial frequency of the adapting stimuli. Arnold et al. (2016) and Lee and Chong (2021) previously employed dynamic noise patterns that predominantly leaned towards the low spatial frequencies, which are notably favored by the M pathway in comparison to higher spatial frequencies. Therefore, we aimed to understand how contrast discrimination following FFAd would differ when adapting stimuli primarily contained low spatial frequencies versus high spatial frequencies.

We hypothesized that adapting stimuli with low spatial frequencies would adapt the M pathway more effectively than high spatial frequencies, leading to higher Δ*C*s for lower spatial frequency test conditions and possibly lower Δ*C*s for higher spatial frequency test conditions. To test this, we compared images filtered through low-pass (M-biased) and band-pass (P-biased) methods. Considering the M pathway's inclination towards low spatial frequencies, it is logical to assume that noise patterns emphasizing these frequencies, while minimizing the higher ones, might result in a more pronounced adaptation effect on the M pathway.

To assess the influence of adapting spatial frequencies of the flicker on ΔCs for test stimuli across different spatial frequencies, we deviated from the design of Experiment 1 by extending the range of spatial frequencies tested with the Gabor patch to include 0.5, 1, 2, and 4 cpd. Additionally, we adjusted the pedestal contrast levels of the test stimuli to 10% and 30%. Furthermore, in Experiment 1, we employed flicker adaptation with adapting stimuli maintaining

a constant configuration while only their luminance values were updated, akin to the methodology used by Arnold et al. (2016). Such an approach may be prone to generate afterimages. To address this concern, in Experiment 2, we introduced drift in random directions in the low-pass and band-pass filtered images matching the speed of the flicker's temporal frequency (10.6 Hz).

Method

Stimuli. Four adapting stimuli conditions were employed: NS-S (No Spatial Frequency, Static), NS-F (No Spatial Frequency, Flickering), LS-F (Low Spatial Frequencies, Flickering), and HS-F (High Spatial Frequencies, Flickering). The configurations for NS-S and NS-F were congruent with the 0C-S (0% Contrast, Static) and 0C-F (0% Contrast, Flickering) conditions, respectively, as established in Experiment 1.

For the generation of patterns in low and high spatial frequencies, we started by crafting 280 random white noise patterns, each having a circular shape with an 8.2° diameter. These noise images were first processed using a two-dimensional Fast Fourier Transform (FFT) to convert them to the frequency domain. Subsequent to this, a spatial filter was applied. Gaussian filters were used to target either the low or high spatial frequencies. The low-pass filtered stimuli exhibited a power spectrum that peaked at lower spatial frequencies, steeply tapered off at around 2.5 cpd with a standard deviation (σ) of 9. Conversely, the band-pass filtered stimuli demonstrated a peak power at 5 cpd, with a notable reduction in power at spatial frequencies both below and above this peak. The band-pass patterns were generated using a Difference of Gaussians approach, setting the lower and upper cutoff frequencies at standard deviations (σ) of 0.8 and 1.3, respectively. To ensure a seamless integration of the pattern edges with the targeted spatial frequencies, these stimuli were modulated within a Gaussian window.

Figure 7 provides illustrative examples of both types of spatially filtered patterns and their power spectra. The upper left image is a Gaussian low-pass filtered patch, demonstrating a homogenous distribution of grayscale intensities with a gradual transition from light to dark, indicative of attenuation of higher spatial frequencies. Below, the band-pass filtered patch exhibits a more distinct texture, reflecting a selective frequency range. The power spectrum for the low-pass filtered image (upper right graph) shows a concentration of power within the low spatial frequencies, predominantly below 15 cycles per image (cpi), which equates to 2 cpd when adjusted for the experimental viewing conditions. Conversely, the power spectrum for the band-pass filtered image (lower right graph) peaks at approximately 50 cpi (6.3 cpd), suggesting that this filter allows frequencies within a specific mid-to-high range while filtering out others.

In determining contrast levels, we standardized all adapting patterns to a 20% Michelson contrast. To achieve this, luminance values were sampled at the 10th percentile (L_{min}) and the 90th percentile (L_{max}.). This sampling method was employed to minimize the influence of extreme luminance outliers. By integrating these sampled values with the predetermined 20% Michelson contrast criterion, we meticulously adjusted the contrast of each pattern.

In terms of the patterns' drift and temporal frequency, patterns were devised to present a drifting motion in random directions, aligning with the flicker's temporal frequency to eliminate afterimages to the adapting stimuli. This frequency was set at 10.6 Hz on an 85 Hz monitor. A visual representation of this can be observed in Figure 8. Each row of the figure illustrates a complete cycle comprised of eight frames. The cycle initiates with a newly crafted image (depicted on the far left of each row) and every eighth frame (depicted on the far right of the top row and the left of the bottom row) introduces a new pattern. The intermediate six frames between these key images result from linear interpolation. As the cycle progresses, frames that

appear early bear a stronger resemblance to the cycle's initial pattern, whereas the later frames take on the characteristics of the subsequent cycle's beginning pattern. By the midpoint of the transition, the patterns closely mirror the average of the two anchoring patterns.

In the current experiment, 280 complex patterns were presented in each cycle, repeated over 30 seconds, necessitating highly precise timing controls. To achieve this, the process priority was set to 'realtime' using the ‘core.rush’ function in PsychoPy. This function utilizes the ‘REALTIME_PRIORITY_CLASS’ constant from the ‘psutil’ package (Rodola, 2020), a versatile, cross-platform library designed for system monitoring and management, including process information retrieval and resource utilization (CPU, memory, disks, network, sensors). This setting is crucial for reducing system latencies and ensuring the fidelity of timing measurements.

Furthermore, the display's refresh timing was periodically evaluated (before beginning of and whilst all experiments). This involved recording the precise moment of each refresh interval while cycling through the 280 patterns over a 30-second duration, corresponding to 2250 frames. The exemplary results, illustrated in Figure 9a and 9b, confirm the system's high temporal accuracy, with refresh intervals consistently near the target of 11.76 ms—corresponding to the expected frame duration on an 85 Hz monitor. The intervals recorded were 11.76±0.06 ms for Figure 9a and 11.76±0.16 ms for Figure 9b, demonstrating the system's consistent ability to maintain timing precision with deviations of less than 1 ms across multiple tests.

For our test stimuli, we examined four spatial frequencies (0.5, 1, 2, and 4 cpd) of the Gabor patch at two pedestal contrast levels (10% and 30%). This was done to investigate the FFAd effects that the spatial frequencies of adapting stimuli might differentially have on contrast discrimination (ΔC) across different spatial frequencies following adaptation. All other

specifications for the adapting and test stimuli and the procedure remained consistent with those detailed in Experiment 1.

Design and Analysis. Our approach to design and analysis closely paralleled that of Experiment 1. However, a distinct difference was our emphasis on evaluating the spatial frequencies of both adapting and test stimuli, as opposed to focusing on contrast as we did in Experiment 1. For data analysis, we utilized a three-way repeated measures ANOVA, considering factors of spatial frequency for adapting stimuli (4 levels), pedestal contrast for test stimuli (2 levels), and spatial frequency for test stimuli (4 levels).

Results

A three-way repeated measures ANOVA conducted on the increment threshold (ΔC) data for Experiment 2 revealed a significant main effect for test pedestal contrast, $F(1, 8) = 168.43$, $p < .001$, $\eta^2 = .494$. This difference is illustrated in Figure 10a, where the black line (30% test pedestal contrast) and the gray line (10% test pedestal contrast) show a clear difference. There was no significant main effect for adapting conditions [$F(3, 24) = 1.77$, $p = .179$, $\eta^2 = .008$] and for test spatial frequency [$F(3, 24) = 0.352$, $p = .788$, $\eta^2 = .006$]. There were no significant interaction effects among the variables. Our hypothesis was that adapting flicker with low spatial frequencies would more effectively adapt the M pathway. Thus, we expected higher ΔCs in lower spatial frequency test conditions and potentially lower ΔCs in higher spatial frequency test conditions; however, these effects were not observed.

Additionally, the effect of temporal adapting flicker on contrast discrimination was not evident, as no flicker effect with uniform pattern (0C-F condition) was detected in Experiment 1 under contrast discrimination conditions involving higher test pedestal contrasts. Figure 10b presents the same data as Figure 10a designed to show a clear comparison between the results of

Experiments 1 and 2. In Experiment 2, the NS-S and NS-F conditions correspond to the 0C-S and 0C-F conditions from Experiment 1, representing the static uniform pattern condition and the uniform pattern flicker condition, respectively. Comparing both adaptation conditions from both experiments at 10% and 30% test pedestal contrasts and the lowest (0.5 cpd in both experiments) and highest (4 cpd in Experiment 2 and 5 cpd in Experiment 1) test spatial frequencies revealed no differences [$F(1, 8) = 1.097$, $p = .326$, $\eta^2 = .008$], indicating consistent results between the experiments.

Discussion

The effect of FFAd (NS-F, LS-F, and HS-F conditions) on contrast discrimination was not evident in the current experiment. The NS-F condition, which involved a uniform pattern flicker, was identical to the 0C-F condition from Experiment 1. The results of the NS-F condition were consistent with the findings from Experiment 1, where no FFAd effect was observed under contrast discrimination tasks involving higher test pedestal contrasts.

Our hypothesis that adapting flicker with low spatial frequencies (LS-F condition) would more effectively decrease contrast response mediated by the M pathway than other conditions was not supported, as there was no significant difference in ΔCs. There might be three main reasons for these results:

1. Contrast level of adapting flicker: The average contrast level of each pattern of adapting flicker was 20%, which might not be sufficient to decrease the contrast response of M cells (increase contrast discrimination thresholds), given our results in Experiment 1. In Experiment 1, at a test pedestal contrast of 30%, only adapting flicker with 50% contrast was effective. The uniform pattern flicker condition (temporal modulation only) was effective only at a test pedestal contrast of 0% (detection thresholds), not at higher test contrasts (discrimination

thresholds).

2. Measurement of only contrast discrimination thresholds: Unlike in Experiment 1, in Experiment 2 we measured only contrast discrimination thresholds. If we had measured contrast detection thresholds as well, we might have obtained supportive results.

3. Induced random direction motion perception: An inconsistent finding between the two experiments was that at a 10% test pedestal contrast, 10% contrast adapting flicker was effective in Experiment 1, unlike in this Experiment 2, with 20% contrast adapting flicker. This might be because our flicker stimuli likely induced random direction motion perception in addition to the temporal luminance modulation of flicker. To isolate the flicker adaptation effect while minimizing spatial aftereffects, we employed a method where different patterns were updated at the peaks and troughs of a sine wave, matching the temporal modulation of the flicker, with linear interpolation between these points. This approach likely resulted in perceived random motion during flicker adaptation. Observers' verbal reports confirmed their perception of motion in the adapting flicker.

The random directions of the moving elements within the flicker pattern might not effectively adapt the M cells. Targeting specific groups of M cells with motion in a consistent direction could potentially be more effective for adaptation. Traditional motion aftereffect studies conventionally have used motion in one direction over an adaptation duration of 30 seconds (e.g., Bartlett et al., 2018; Huk et al., 2001; Murd & Bachmann, 2011; Nishida & Ashida, 2000; van de Grind et al., 2004). To adapt various groups sensitive to different directions effectively, the adaptation duration might need to be significantly longer, or alternatively, using adapting flicker that moves in a single direction might be more effective during a 30-second period.

Experiment 3: The Impact of Temporal Frequency in Adapting Flicker on Contrast Discrimination.

Results from Kaneko et al. (2015) and Ye et al. (2021), who employed spatially uniform patterns, align closely with the 8 to 12 Hz frequency range where the human visual system shows peak sensitivity. Specifically, Kaneko et al. (2015) reported a significant shift in perceived spatial frequency at 8 Hz, contrasting with results at 4 and 16 Hz. In a similar vein, Ye et al. (2021) found the FFAd effect to be dominant at 12.5 Hz, with no observable effect at 60 Hz. Additionally, the optimal temporal frequencies for activating the M cells in the macaque LGN are reported to be higher, around 20 Hz (Derrington & Lennie, 1984; Hicks et al., 1983; Solomon et al., 2004). These findings collectively suggest that temporal frequencies in the range of 10 to 20 Hz are likely most effective for adapting the M pathway.

Arnold et al. (2016) and Lee and Chong (2021) attributed their observations to the adaptation of the M pathway, sensitive to low spatial frequencies, by nearly imperceptibly high temporal frequencies, resulting in increased sensitivity to higher spatial frequencies. Yet, it is likely their temporal frequencies deviated from their intended target frequencies (Figure 4). If they had accurately achieved their desired temporal frequency with dynamic noise patterns as adapting flicker stimuli, their findings could have mirrored those of Kaneko et al. (2015) and Ye et al. (2021). Notably, none of these studies examined adapting stimuli conditions with spatial components flickering at varying temporal frequencies with precise temporal modulations.

Another possible interpretation of their results suggests that the temporal domain of the adapting stimuli used by Arnold et al. (2016) and Lee and Chong (2021) may have exerted only a

marginal impact on their findings. The enhanced sensitivity to higher spatial frequencies might be attributed to spatial aftereffects, stemming from a consistent spatial structure characterized by low spatial frequencies, rather than from the temporal flicker. To explore this possibility further, a comparison between static adapting stimuli and those with moving components at the desired temporal frequency would be insightful.

In Experiment 3, we assessed adapting stimuli at multiple temporal frequencies (0, 2.5, 10.6 Hz, and 21.3 Hz), integrating spatial components of contrast and spatial frequency. Considering the M pathway's higher contrast gain at lower contrasts and its preference for low spatial frequencies, we set the contrast at 20% and employed low-pass filtered patterns.

Our hypotheses were, first, we anticipated that adapting stimuli, comprising temporally modulated low-pass filtered patterns with drifting spatial components, would not produce spatial aftereffects. If the results from adapting flicker stimuli (characterized by low spatial frequencies and absence of spatial aftereffects) were similar to or exceeded the effects of static low-pass filtered patterns, which are presumed to induce spatial aftereffects, it would indicate that temporal flicker accompanied by spatial elements can effectively drive the FFAd effect on spatial vision. Specifically, we expected that static adapting stimuli with low spatial frequencies would adapt the M pathway (low spatial frequency channel) and decrease contrast discrimination at low spatial frequencies of test stimuli (resulting in higher ΔCs).

We predicted that the FFAd effect would be pronounced at 10.6 Hz or 21.3 Hz. The adapting stimuli, characterized by low contrasts and low spatial frequencies combined with moderately high temporal frequencies, are likely optimally designed to adapt the M pathway. The choice of 10.6 Hz is based on its alignment with peak human sensitivity, as the temporal contrast sensitivity curve peaks around 10 Hz and diminishes at frequencies both above and

below this point (de Lange Dzn, 1958; Kelly, 1961, 1972; Kulikowski & Tolhurst, 1973; Lloyd & Landis, 1960; Regan, 1968). This finding is supported by studies such as those by Kaneko et al. (2015) and Ye et al. (2021), which identified the highest FFAd effects near 10 Hz. Conversely, the choice of 21.3 Hz corresponds closely to the 20 Hz at which macaque M LGN cells exhibit their highest activity, suggesting another potential peak for FFAd effects. Building on these insights, we also hypothesized that temporally modulated flickers at a frequency of 2.5 Hz might produce weaker effects, given that this frequency is significantly slower than the 10 Hz peak associated with optimal human temporal sensitivity. This lower frequency may not engage the M pathway as effectively, potentially resulting in less pronounced adaptation effects.

For the static adapting condition (0 Hz) in Experiment 3, we incorporated a low-pass filtered pattern to determine if the flicker conditions could produce adaptation effects that are comparable to or greater than the spatial aftereffects observed.

Method

Stimuli. We chose four temporal frequency conditions for the adapting stimuli: 0 (static), 2.5, 10.6, and 21.3 Hz. The baseline condition consisted of a static, low-pass filtered image. For the other temporal frequency conditions, the mean luminance was modulated sinusoidally at the specified frequency, and the spatial components moved at the same rate. We employed low-pass filtered patterns for spatial configurations, consistent with the low-pass filtered images used in Experiment 2. The conditions for the test stimuli remained identical to those in Experiment 2.

Design and Analysis. The design and analytical approach adopted in this experiment was akin to that of Experiment 2. Data analysis was conducted using a three-way repeated measures ANOVA. The factors considered were temporal frequency of adapting stimuli (4 levels), pedestal contrast of test stimuli (2 levels), and spatial frequency of test stimuli (4 levels).

Results

A three-way repeated measures ANOVA conducted on the increment threshold (ΔC) data from Experiment 3 identified significant main effects for the temporal frequency of the adapting flicker, $F(3, 24) = 4.15$, $p = .017$, $\eta^2 = .024$, as depicted in Figure 11a, and for test pedestal contrast, $F(1, 8) = 330.12$, $p < .001$, $\eta^2 = .578$, as shown in Figure 11b. The main effect of test spatial frequency was not significant, $F(3, 24) = 0.406$, $p = .750$, $\eta^2 = .010$. There were no significant interaction effects among the variables, with the exception of a marginally significant interaction between the temporal frequency of the adapting flicker and test pedestal contrast, $F(3, 24) = 2.767$, $p = .064$, $\eta^2 = .023$. Figure 12 presents a clearer comparison between the results of all three experiments, using the same data as shown in Figure 11b.

Based on these findings, subsequent pairwise comparisons were conducted using two-tailed tests with adjustments for multiple comparisons through the Benjamini-Hochberg procedure, due to the significant main effects observed for the temporal frequency of the adapting flicker. Averaging across test pedestal contrast conditions, significant differences were identified at a test spatial frequency of 0.5 cpd. Specifically, the 0 Hz adapting condition differed significantly from the 2.5 Hz, 10.6 Hz, and 21.3 Hz conditions (all yielded $p = .050$), as illustrated in Figure 11a. It is important to note that for the static adapting condition (0 Hz) in Experiment 3, a low-pass filtered pattern was used to evaluate whether the flicker conditions could induce adaptation effects comparable to those observed with spatial aftereffects. Unlike the uniform pattern featured in the static adapting condition of Experiments 1 and 2, the 0 Hz condition in Experiment 3 used a low-pass filtered image with 20% average contrast.

Given that the 0 Hz adapting condition in Experiment 3 significantly differed from the 2.5 Hz, 10.6 Hz, and 21.3 Hz conditions, we extended our investigation to examine its distinction

from the uniform pattern static condition used in earlier experiments. Given that the low spatial frequency was consistently 0.5 cpd across all experiments, and the high spatial frequency was set at 5 cpd in Experiment 1 and 4 cpd in Experiments 2 and 3, we focused on the consistent conditions in Experiment 2 and 3 for further analysis. Therefore, we conducted a three-way repeated measures ANOVA to compare the two static adapting conditions—the uniform pattern from Experiment 2 and the low-pass filtered pattern from Experiment 3—across two test pedestal contrasts (10% and 30%) and two levels of test spatial frequency (0.5 cpd and 4 cpd).

The analysis revealed a significant interaction among the static adapting conditions, test spatial frequencies, and test pedestal contrasts, $F(1, 8) = 5.447$, $p = .048$, $\eta^2 = .056$. Further pairwise comparisons, adjusted using the Benjamini-Hochberg procedure, identified a significant difference between the uniform and low-pass filtered patterns at 4 cpd ($p = .040$) and a marginally significant difference at 0.5 cpd ($p = .089$) when the test pedestal contrast was set at 10%, as shown in Figure 13a. This marginal difference at 0.5 cpd reached significance ($p = .026$) when comparing data across Experiments 1 and 2 with those from Experiment 3.

We also extended our analysis to compare the static adaptation condition with a uniform pattern from Experiment 2 against the other adapting conditions used in Experiment 3. This comparison aimed to align the results with those observed in Experiments 1 and 2. Consistent with the results from Experiment 2, this analysis revealed no significant differences among the various adapting conditions, with the exception of a significant effect related to the test pedestal contrast variable, $F(1, 8) = 52.026$, $p < .001$, $\eta^2 = .501$. The findings from this comparison are presented in Figure 13b.

Discussion

We observed that the static low-pass filtered pattern with 20% average contrast resulted

in higher Δ*C*s, particularly at a 0.5 cpd test spatial frequency and 10% test pedestal contrast, compared to the flicker adapting conditions (2.5 Hz, 10.6 Hz, and 21.3 Hz). Additionally, when compared with the static uniform pattern adapting condition from Experiment 2, there were no significant differences in Δ*C*s among the various adapting conditions. This aligns with the findings from Experiment 2.

These results suggest that the low-pass filtered patterns with moving elements, used in both Experiments 2 and 3, may not effectively induce adaptation in the M pathway. However, when the same low-pass filtered pattern was presented continuously as a static 0 Hz condition with consistent spatial contrasts and frequencies, it was sufficient to produce a significant adaptation effect. Notably, the flicker adapting conditions involved dynamically updating patterns on a per-frame basis, which might preclude a direct comparison with the static low-pass filtered adaptation. For more conclusive comparisons of spatial aftereffects and flicker adaptation effects in subsequent studies, it might be beneficial to employ consistent patterns across all adapting conditions, varying only in temporal luminance modulation for flicker conditions.

Interestingly, when comparing the static adapting conditions between the uniform pattern from Experiment 2 and the low-pass filtered pattern from Experiment 3, a significant difference was observed at 4 cpd. As shown in Figure 13a, the Δ*C*s for the static low-pass filtered pattern adapting condition at 10% test pedestal contrast for a test spatial frequency of 4 cpd were lower than those for the static uniform pattern adapting condition. These results suggest that the spatial aftereffects, specifically the increased Δ*C*s at low test spatial frequencies induced by the low-pass filtered pattern, indicate adaptation within the M pathway. Additionally, these aftereffects might also reflect an antagonistic interaction between the M and P pathways. Specifically, the decreased ΔCs at high test spatial frequencies could indicate an enhanced contrast response in

the P pathway, potentially resulting from decreased activity in the M pathway. Consistent effects were observed in Experiment 1 (refer to Figure 6a) at 10% test pedestal contrast at the high spatial frequency condition (5 cpd). Further theoretical insights into the antagonistic interactions between the M and P pathways are discussed in reviews by Brown (2018) and Weisstein et al. (1992), as well as in the general discussion section of the current study.

General Discussion

The spatiotemporal dimensions of vision and their association with the M and P pathways have been predominantly studied in the context of immediate phenomena, such as visual masking. However, long-term adaptation phenomena, such as Fast Flicker Adaptation (FFAd), have not been as thoroughly explored. This study aimed to bridge this gap by investigating the effects of FFAd and identifying its influencing factors through a series of experiments (Experiments 1, 2, and 3).

In Experiment 1, we observed a FFAd effect with uniform pattern flicker at 10.6 Hz on contrast sensitivity at the low (0.5 cpd) spatial frequency, consistent with the previous findings from Kaneko et al. (2015). Also, as we expected, we found that contrast plays a significant role in FFAd effects, impacting both contrast sensitivity (detection) and contrast response (discrimination). Adapting flicker with higher contrasts led to increased Δ*C*s in tasks assessing contrast detection and discrimination at low spatial frequencies. This consistent trend of ΔCs across different test pedestal contrasts further supports the efficacy of the contrast response function as a robust measure of M pathway function, alongside the contrast sensitivity function.

Notably, as shown in Figure 6a, differences in averaged Δ*C*s at low spatial frequencies for the adapting flicker contrast conditions were visually more pronounced at higher test pedestal contrasts (30% and 50%). However, despite these apparent differences, the statistical analysis revealed stronger significance for the differences at lower test pedestal contrasts (0% and 10%), as indicated by lower p-values. This observation suggests FFAd might be particularly effective in reducing the high contrast gain of the M pathway at low contrasts. The observed decrease in Δ*C*s

following FFAd at a 10% test contrast in the 5 cpd condition supports this. The reduced activity in the M pathway might have led to enhanced sensitivity in the P pathway for low contrast discrimination.

Consistent findings were observed when comparing the static uniform pattern adapting condition from Experiment 2 with the static low-pass filtered pattern adapting condition from Experiment 3. At a low spatial frequency and a low contrast (10%), Δ*C*s tended to be higher following adaptation to the static low-pass filtered pattern than to the static uniform pattern. Conversely, at a high spatial frequency, under the same test contrast conditions, this pattern reversed; ΔCs were lower after adaptation to the static low-pass filtered pattern.

The observed enhancement in contrast discrimination at the high spatial frequency may be attributed to the antagonistic release of P pathway activity, potentially in response to adaptation in the M pathway. This phenomenon aligns with the theory of antagonistic interactions between the M and P pathways, which suggests a functional rebalancing where decreased activity in one pathway leads to increased activity in the other (for reviews, see Brown, 2018; Weisstein et al., 1992). Support for this theory can also be found in visual masking research, particularly metacontrast studies, which demonstrate how the M pathway's transient activity inhibits the P pathway’s sustained activity (Breitmeyer, 2007; Breitmeyer & Öğmen, 2006). Our findings may represent another instance of these antagonistic interactions, where adaptation in the M pathway due to prolonged flicker exposure leads to enhanced P pathway activity.

Although we found the effect of contrast in adapting flicker, this finding warrants further investigation, particularly concerning different modulation depths which were not compared in our experiments. In our efforts to assess the effects of contrast, we maintained a fixed mean

luminance for each spatial pattern. However, to introduce contrast while preserving mean luminance, our stimuli inevitably exhibited varying maximum and minimum luminance levels across contrast conditions. Specifically, the adapting condition with higher contrast displayed higher and lower absolute luminance values in the inner and outer circles, respectively, compared to lower contrast conditions. Although our results likely reflect the effect of contrast —particularly as the boundary between the inner circle and the outer circle of the adapting flicker pattern was aligned with the central part of each test Gabor patch—it remains possible that the observed enhanced FFAd effect was influenced not only by higher contrast but also by the inclusion of higher absolute luminance values in the flicker conditions. Future studies should isolate these variables to definitively determine their individual contributions to FFAd effects.

In Experiments 2 and 3, no significant effects of spatial frequency components (Experiment 2) or temporal frequency (Experiment 3) of adapting flicker on contrast discrimination were observed. These results warrant further investigation into these factors. Notably, our stimuli in Experiments 2 and 3 did not include optimal contrast levels and incorporated motion in random directions, which may not sufficiently adapt M cells within the brief adaptation period of 30 seconds.

An adapting stimulus that flickers and drifts in a single direction may more effectively adapt the M cells. Breitmeyer (1973) examined the effects of motion stimuli moving in one direction and discovered that the greatest increase in detection threshold occurred with low spatial frequency (0.4 cpd) test gratings after adapting to a rapidly moving texture pattern from right to left at a velocity of 6.5 dps for 2 minutes. This effect was more pronounced than the increase observed with high spatial frequency (10.5 cpd) test gratings after adapting to a slowly drifting pattern. His results indicate that the effects of spatial and temporal frequencies in

randomly directed adapting flicker could be significant if the motion is unidirectional. The findings from Experiment 1 suggest that these adapting stimuli should have high contrast. Therefore, future research should focus on using low spatial frequency and high contrast images that flicker while moving in one direction at high speeds. Such modifications could improve adaptation effects and provide more definitive conclusions about how spatial and temporal properties of adapting flicker influence contrast discrimination.

We did not separately investigate the adaptation effects of flicker and motion, assuming their effects could be additive. However, their interaction might diminish the extent of this additive effect. Erlikhman et al. (2019) studied the interactions between flicker and motion using flicker-induced motion experiments. They observed that these interactions were strongest in the peripheral vision and at flicker frequencies at 15 Hz. Thus, future research should aim to isolate these effects to more clearly understand their influence on contrast discrimination.

Participants reported that they hardly perceived the temporal modulation (overall luminance change of the flicker) of the adapting pattern, in contrast to the visibility of such modulation in the background. This phenomenon may be analogous to motion silencing, where rapid movement within collective motion causes objects undergoing changes in color, luminance, size, or shape to appear static (Burr, 2011; Choi et al., 2016; Peirce, 2013; Suchow & Alvarez, 2011; Turi & Burr, 2013).

Suchow and Alvarez (2011) and Burr (2011) have suggested that the motion integration process is so powerful to override all dynamic signals within a given area, not limited to directional motion but also encompassing changes related to color, size, or shape. According to this framework, the motion in our stimuli could have obscured the participants' ability to process the overall luminance modulation of the flicker, suggesting a possible motion silencing effect.

However, attributing our findings to motion silencing requires caution. Motion silencing is typically observed in peripheral vision and does not generally occur near the point of fixation. Conversely, in our experiment, elements moved randomly, particularly within the central visual field. Additionally, the mechanisms underlying motion silencing are not fully understood, and the conditions necessary for its induction remain less explored. For instance, while Turi and Burr (2013) suggest that a combination of motion and visual crowding might facilitate this effect, Peirce (2013) contends that neither motion nor coherent changes alone are sufficient conditions for inducing silencing.

In conclusion, FFAd represents a promising approach for investigating the function of the M pathway and its interactions with the P pathway. Temporal uniform pattern flicker effectively induces adaptation effects; however, flicker with higher contrast elicits a more pronounced impact on both contrast sensitivity and response. The contrast response function, derived from contrast discrimination tasks, provides a comprehensive view of their respective functions, complementing the insights gained from the contrast sensitivity function obtained through contrast detection tasks. Collectively, these findings highlight the potential of FFAd as a tool for advancing our understanding of spatiotemporal visual processing dynamics.

Table 1: Studies of the Effects of Flicker Adaptation on Spatial Vision

	Adapting Flicker Rate	**Adapting Flicker: Spatial Configuration**	**Adaptation Period**	**Measurement**	**Result**
Arnold et al. (2016)	- 75 Hz (Exp. 1) - 60 Hz (Exp. 2) - 75 Hz (Exp. 3) - 0.8, 120 Hz (Exp. 4)	- Dynamic noise pattern	- 10 seconds on the 1st trial, 5 seconds on the 2nd to 34th trials, and 10 seconds on the 35th trial.	- Face identification: low vs. high pass filtered images (Exp. 1) - Vernier acuity (Exp. 2) - Text (three letters) recognition (Exp. 3) - Contrast sensitivity: constant-size (varied cycles) Gabor patches (Exp. 4)	- Face perception biased toward higher spatial frequencies (Exp. 1) - Vernier acuity improved (Exp. 2) - Sensitivity to lower spatial frequencies diminished at 120 Hz (Exp. 4)
Kaneko et al. (2015)	- 4, 8, 16 Hz (modified Exp. 1 in their Discussion)	- Uniform pattern (upper/ lower half of the screen)	- 1 minute on the 1st trial of a session and 5 seconds on subsequent trials.	- Perceived spatial frequency of constant-size (varied cycles) Gabor patches	- Perceived spatial frequency for 0.25, 0.5, 2 cpd increased at 8 Hz
Lee & Chong (2021)	- 85 Hz (Exp. 1, 2, 3)	- Dynamic noise pattern	- 10 seconds on the 1st trial and 5 seconds on subsequent trials.	- Averaging orientations (Exp. 1) - Averaging sizes (Exp. 2) - Averaging facial expressions (Exp. 3)	- Adaptation increased the precision of averaging orientations, sizes, facial expressions (Exp. 1, 2, 3)
Ye et al. (2021)	- 12.5, 60 Hz	- Uniform pattern (full field)	- 5 minutes after baseline CSF assessment, before retest.	- Contrast sensitivity: bandpass filtered digits (constant-cycle, varied sizes)	- Enhanced sensitivity at CSF peak

Figure 1: Magnocellular (M) and Parvocellular (P) Pathways from the Retina to Cortex

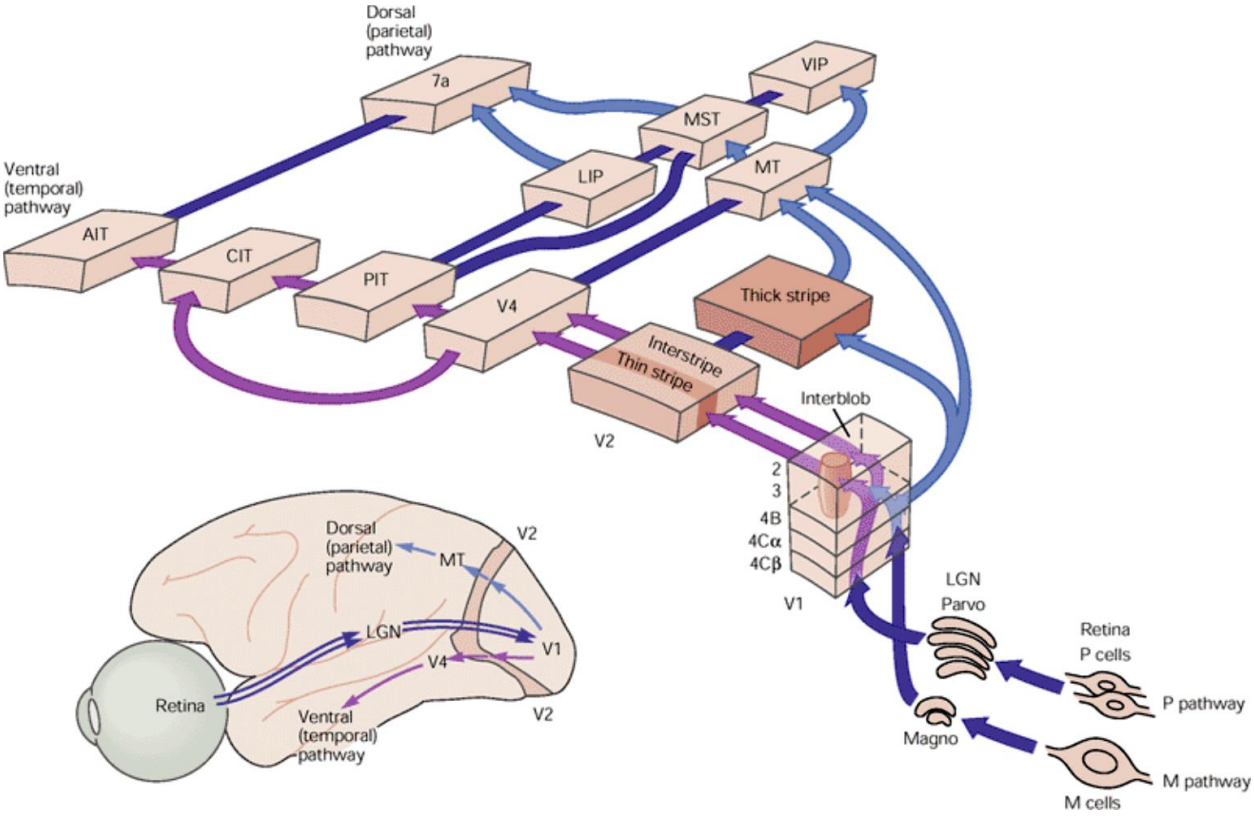

Figure 1. The magnocellular (M) and parvocellular (P) pathways originate in the retina and project through the lateral geniculate nucleus (LGN) to the primary visual cortex (V1). From there, they follow separate pathways through the extrastriate cortex, beginning in V2, and proceed to either the temporal or parietal cortices. The parietal pathway exclusively receives input from the M pathway, while the temporal pathway primarily receives input from the P pathway. In this study, focusing on the earlier areas, we refer to these two distinct pathways as the M and P pathways. Adapted from Kandel et al. (2000). (Abbreviations: AIT = anterior inferior temporal area; CIT = central inferior temporal area; LIP = lateral intraparietal area; Magno = magnocellular layers of the lateral geniculate nucleus; MST = medial superior temporal area; MT = middle temporal area; Parvo = parvocellular layers of the lateral geniculate nucleus; PIT = posterior inferior temporal area; VIP = ventral intraparietal area.)

Figure 2: Comparative Analysis of Contrast Sensitivity Functions for Constant-Size and Constant-Cycle Stimuli

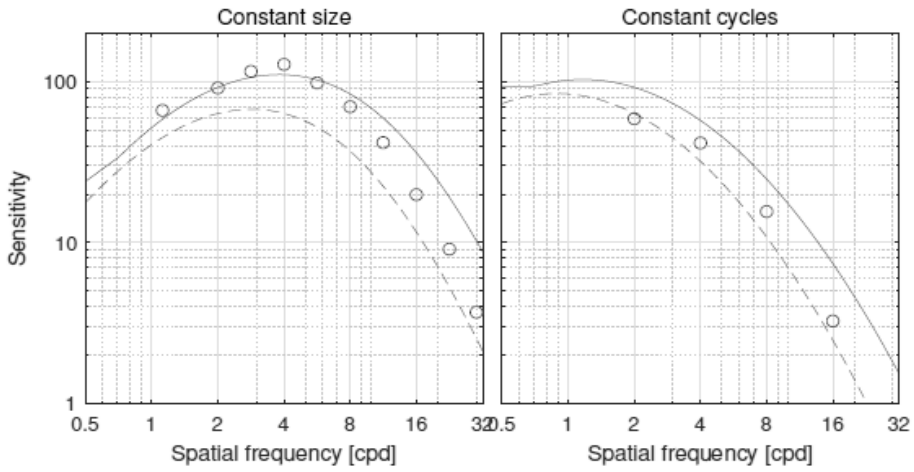

Figure 2. Mantiuk et al.'s (2022) Fig. 8. A CSF using constant-size stimuli (left) exhibits a band-pass shape, peaking around 4 cpd, in line with earlier research like Campbell and Robson (1968). Conversely, a CSF from stimuli with unvarying cycles predominantly displays a low-pass trend, unusually peaking at 1 cpd.

Figure 3: An Example of Dynamic Noise Patterns and Its Associated Power Spectrum

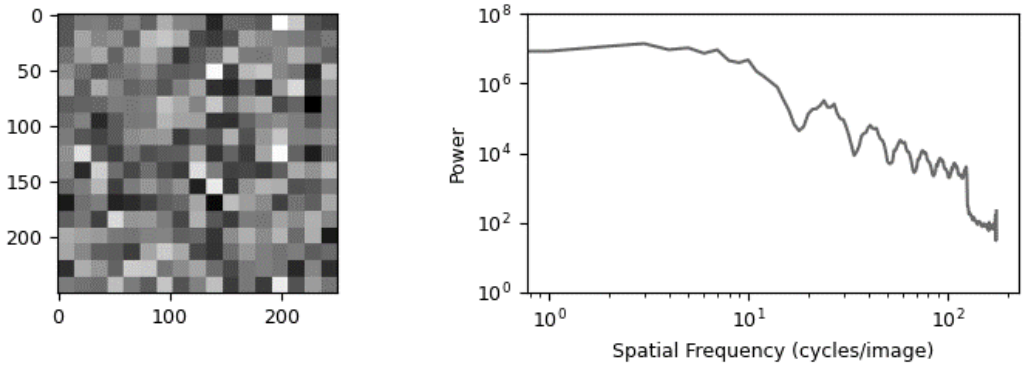

Figure 3. An example of dynamic noise patterns (left) alongside its associated power spectrum (right). The noise pattern is dimensioned at 250 x 250 pixels, and each cell measures 15 x 15 pixels. While the noise pattern integrates square waves spanning multiple spatial frequencies, there is a notable dominance of power within the lower spatial frequencies. If this noise pattern is viewed from a distance of 60 cm, for instance, the power primarily concentrates around 2 cpd and below.

Figure 4: Luminance Modulation Profiles Across Varied Spatial Resolutions in Dynamic Noise Patterns

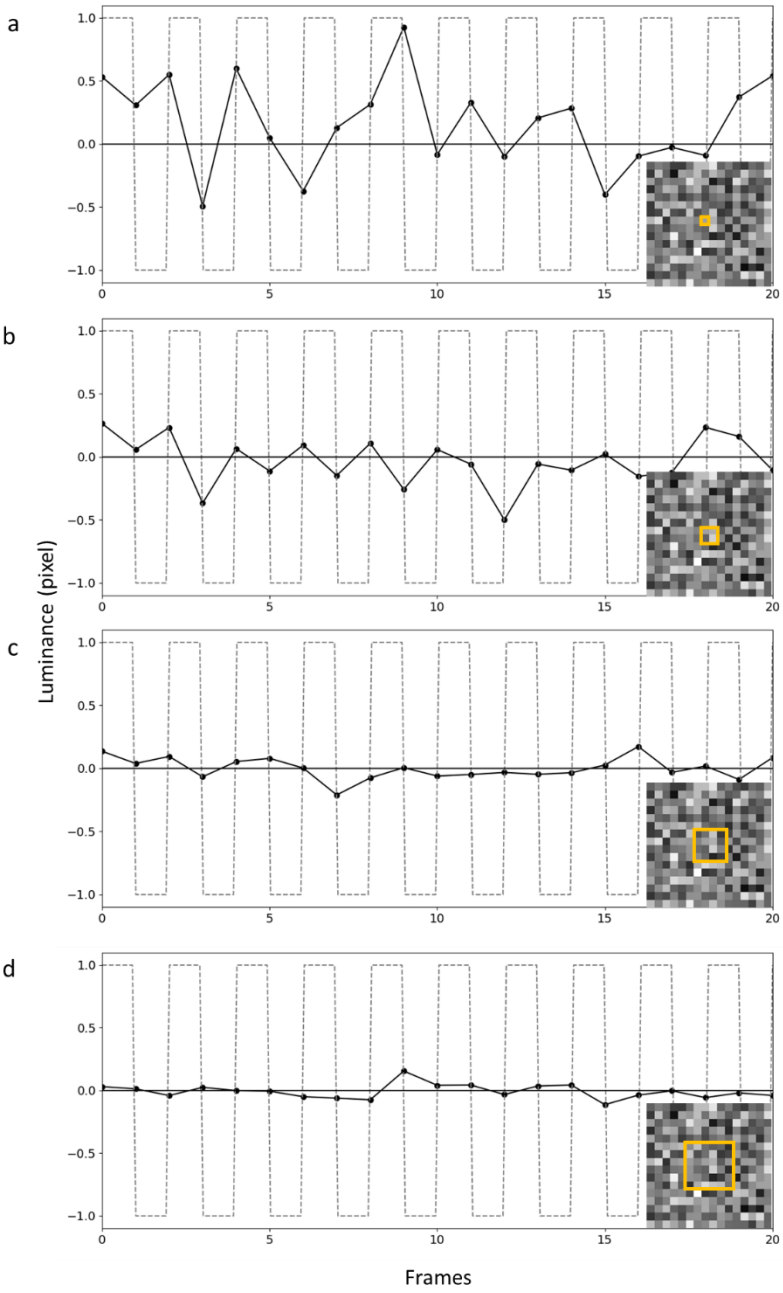

Figure 4. A luminance modulation comparison between a 20-frame square wave (shown by the gray dashed line) and select dynamic noise patterns of different cell sizes as presented by Lee and Chong (2021). The patterns are represented by the black solid line with circles and span: (a) 1 cell (0.2° × 0.2°), (b) 4 cells (0.4° × 0.4°), (c) 16 cells (0.8° × 0.8°), and (d) 36 cells (1.2° × 1.2°). The gray solid line indicates the average luminance of the dynamic noise pattern. With a mean luminance of 127 for the entire image and a standard deviation of 50, individual cells can approach luminance limits of 0 or 255. As the cell area increases, occurrences of back-to-back extreme luminance values lessen, leading to notable decreases in temporal frequencies. For instance, as depicted in (a), a single cell has difficulty matching the frequency of the square wave. By (d), with 36 cells, the curve is almost flat around the mean luminance, highlighting that despite the patterns' rapid updates, achieving a consistent frequency across all conditions remains notably challenging.

Figure 5: Adaptation Stimuli and Procedure in Experiment 1

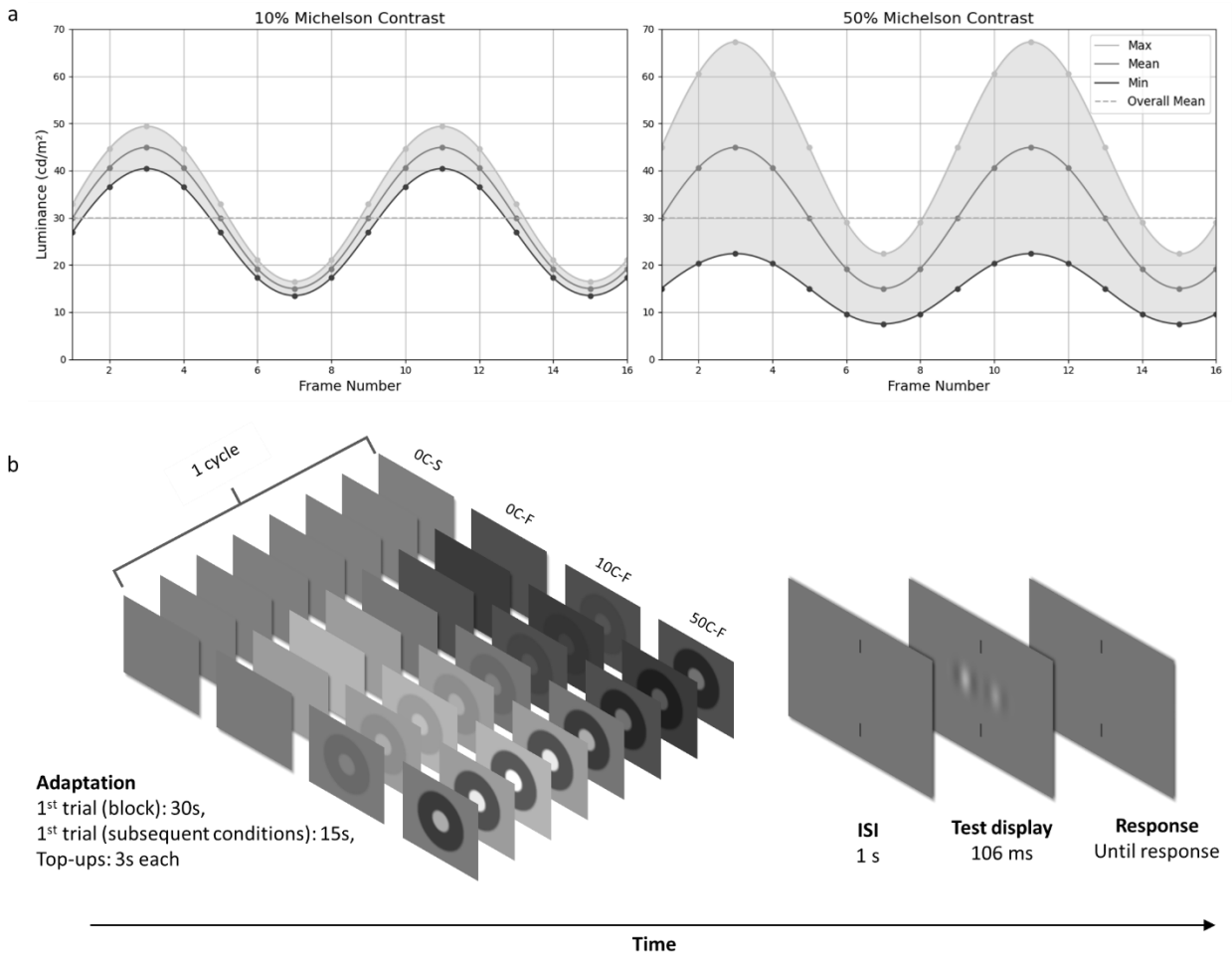

Figure 5. Adaptation Stimuli and Procedure in Experiment 1. (a) Luminance Profiles: The graphs depict the luminance profiles (in cd/m²) over two cycles (16 frames) for conditions 10C-F (10% Michelson contrast, left) and 50C-F (50% Michelson contrast, right) with a 50% temporal modulation on an 85 Hz monitor. The overall mean luminance is indicated by the dashed line (30 cd/m²). The maximum, mean, and minimum luminance values for each stimulus are represented by light, mid, and dark gray lines, respectively, corresponding to the inner circle, background, and outer circle. (b) Experimental Procedure: The schematic illustrates the sequence of the adaptation and test phases for one block of Experiment 1. Each block initiated with a 30-second adaptation to one of four contrast conditions (0C-S, 0C-F, 10C-F, 50C-F), visualized here as eight images representing one complete cycle per condition. Subsequent trials within the block began with a 3-second adaptation top-up, except for the first trial of a new condition, which started with a 15-second adaptation. Following each adaptation, there was a one-second inter-stimulus interval (ISI), punctuated by an auditory cue at the 400 ms mark to signal the presentation of the subsequent test stimulus. The test stimuli were displayed for 106 ms, after which participants were tasked to discern which Gabor patch, left or right, exhibited higher contrast using a two-alternative forced choice (2AFC) method. The illustration shows an example where the left Gabor patch has higher contrast.

Figure 6: Results of Experiment 1

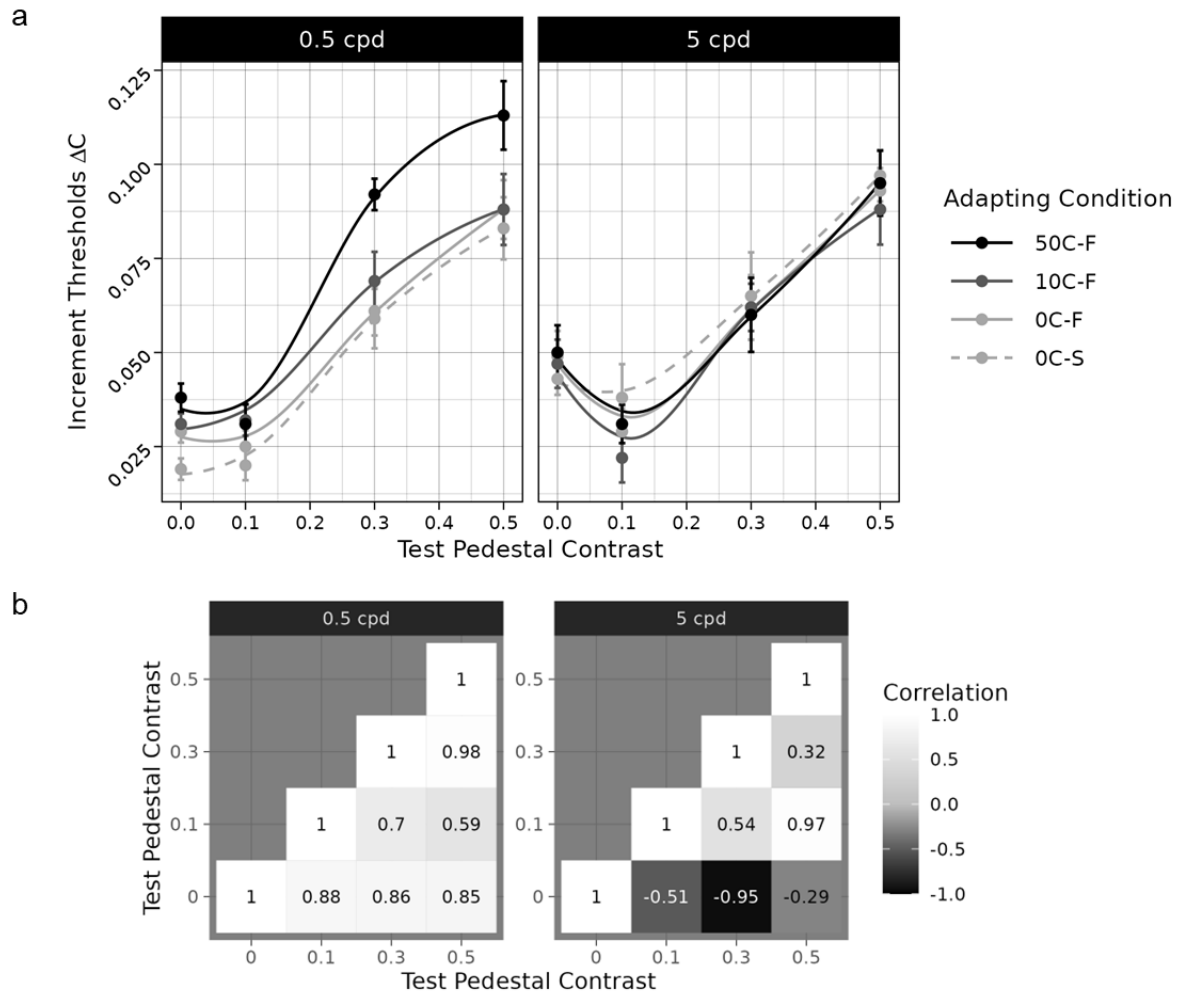

Figure 6. Results of Experiment 1. (a) Contrast response functions (CRFs): Increment thresholds (Δ*C*s) are illustrated for various adapting flicker conditions at two spatial frequencies: 0.5 cpd (left panel) and 5 cpd (right panel). Each panel includes four adapting flicker conditions: 50C-F (50% contrast of adapting flicker, black solid line), 10C-F (10% contrast of adapting flicker, dark gray solid line), 0C-F (0% contrast of adapting flicker, light gray solid line), and 0C-S (0% contrast, static uniform pattern, light gray dashed line). A higher ΔC indicates decreased sensitivity. Notably, at 0.5 cpd, the sequence of decreasing ΔCs from highest to lowest—50C-F, 10C-F, 0C-F, and 0C-S—reflects a sequential decrease in M pathway contrast sensitivity and response in flicker conditions. This pattern is not observed at 5 cpd, which is primarily mediated by the P pathway. Interestingly, all CRF curves except for the static 0C-S show dips at the 10% test pedestal contrast at 5 cpd. (b) Correlation matrix: Pearson's correlation coefficients assessing relationships between ΔCs at different test pedestal contrasts for 0.5 cpd (left panel) and 5 cpd (right panel). Positive correlations are marked in lighter shades, negative in darker shades, with color intensity indicating correlation strength from high (white for strong positive correlations) to low (black for strong negative correlations), with gray representing zero correlation. At 0.5 cpd, the matrix displays strong positive correlations (lighter shades), consistently reflecting the sequence of ΔCs (50C-F highest, followed by 10C-F, 0C-F, and 0C-S lowest). At 5 cpd, this sequence is not maintained, with coefficients ranging from -0.95 to 0.97, highlighting varied interactions at this higher frequency.

Figure 7: Adaptation Stimuli in Experiment 2 and Their Associated Power Spectra

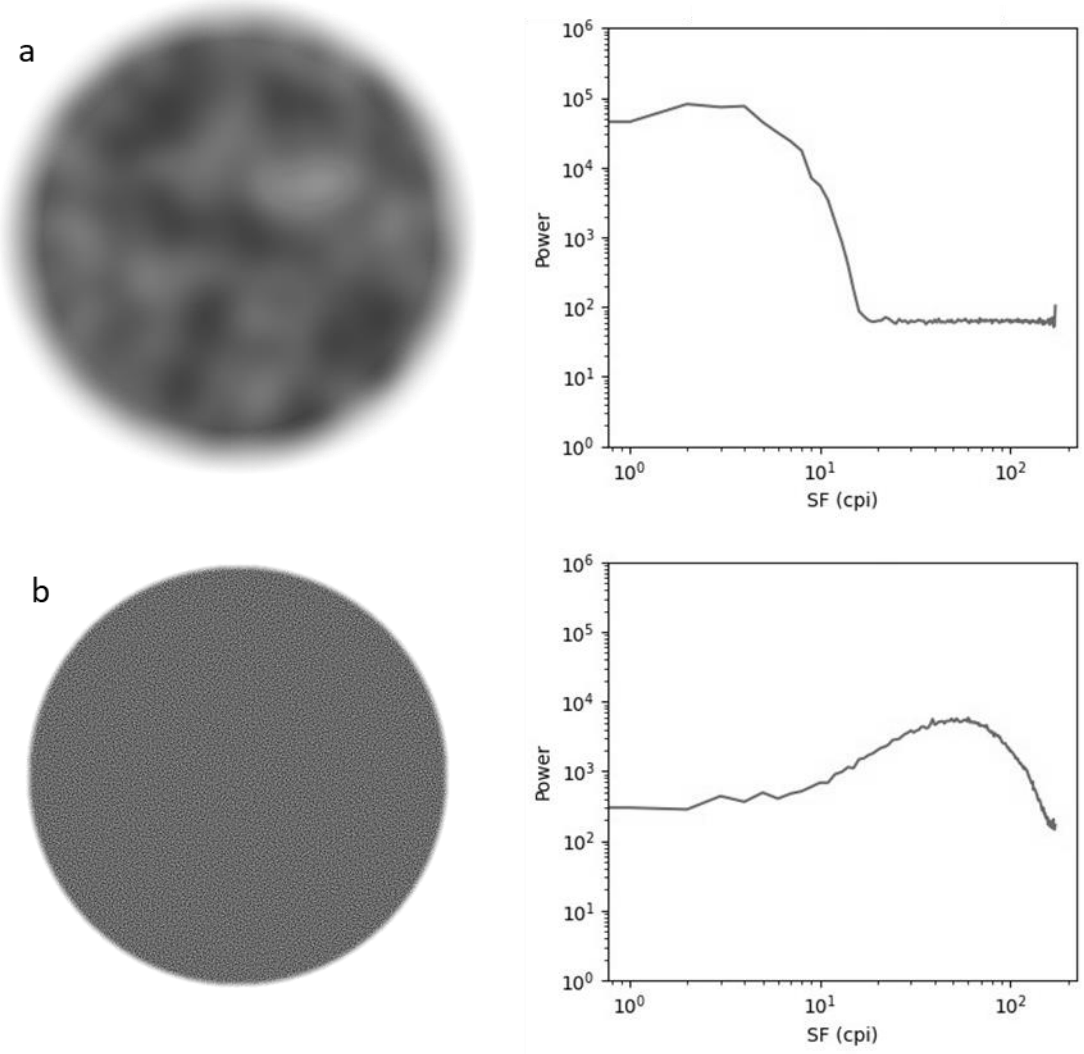

Figure 7. Adaptation stimuli with Gaussian low-pass (top left) and band-pass (bottom left) filtering used in Experiment 2, and their corresponding power spectra (right). The low-pass power spectrum peaks at frequencies below 15 cpi (2 cpd), whereas the band-pass spectrum peaks at around 50 cpi (6.3 cpd), demonstrating the specific spatial frequency ranges tested.

Figure 8: Temporal Progression of Adaptation Stimuli in Experiment 2

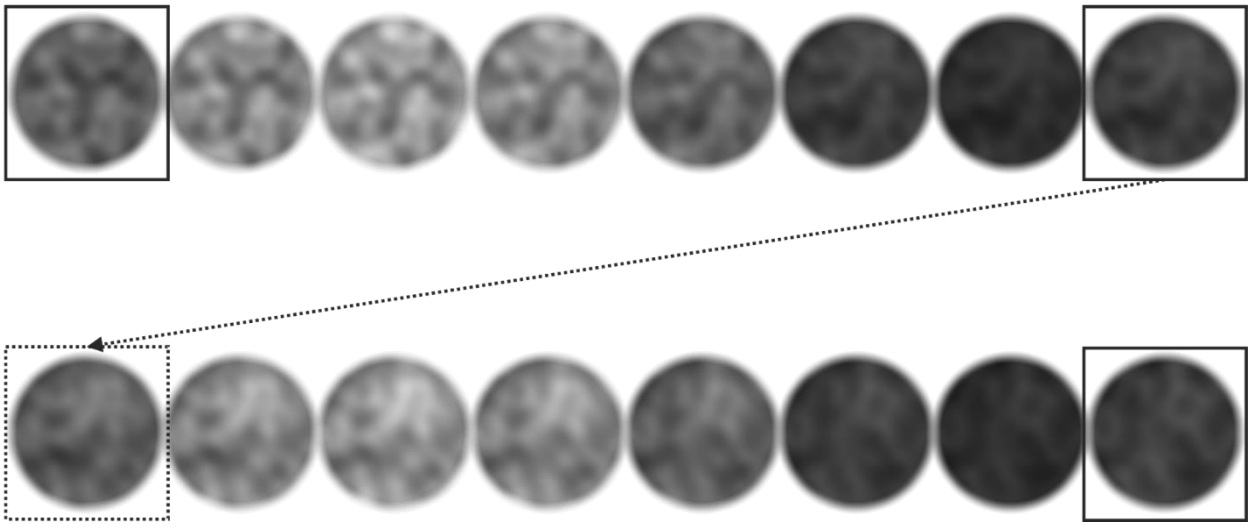

Figure 8. Display of two cycles of frames at 10.6 Hz on an 85 Hz monitor. Each cycle encompasses eight frames. Every eighth frame (surrounded by a solid gray box) showcases a new pattern, with the intermediate frames representing a linear interpolation between the patterns. The progression in each cycle moves from the initial pattern (leftmost image in each row) to the beginning pattern of the subsequent cycle (rightmost image in the top row and leftmost in the bottom row). The central frames, especially the fourth and fifth, depict a blend of the initial and subsequent patterns. The gray dotted line visually separates the two cycles for clarity.

Figure 9: Refresh Intervals Recorded from the Monitor

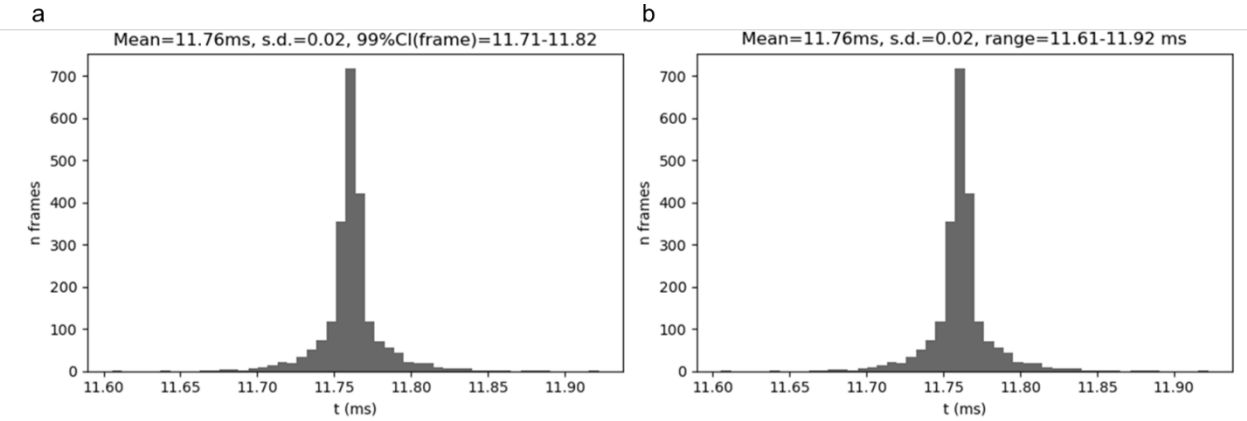

Figure 9. Examples (a, b) of refresh intervals recorded from the monitor used in all experiments. The display's refresh timing was assessed by recording intervals while cycling through 280 patterns over 30 seconds, equivalent to 2250 frames. Histograms (a) and (b) indicate that the refresh intervals for the majority of frames are closely aligned with the expected 11.76 ms—corresponding to the frame duration on an 85 Hz monitor. Specifically, intervals were recorded at 11.76±0.06 ms for (a) and 11.76±0.16 ms for (b), showing the system's capacity to consistently maintain timing precision with deviations of less than 1 ms across multiple tests.

Figure 10: Results of Experiment 2

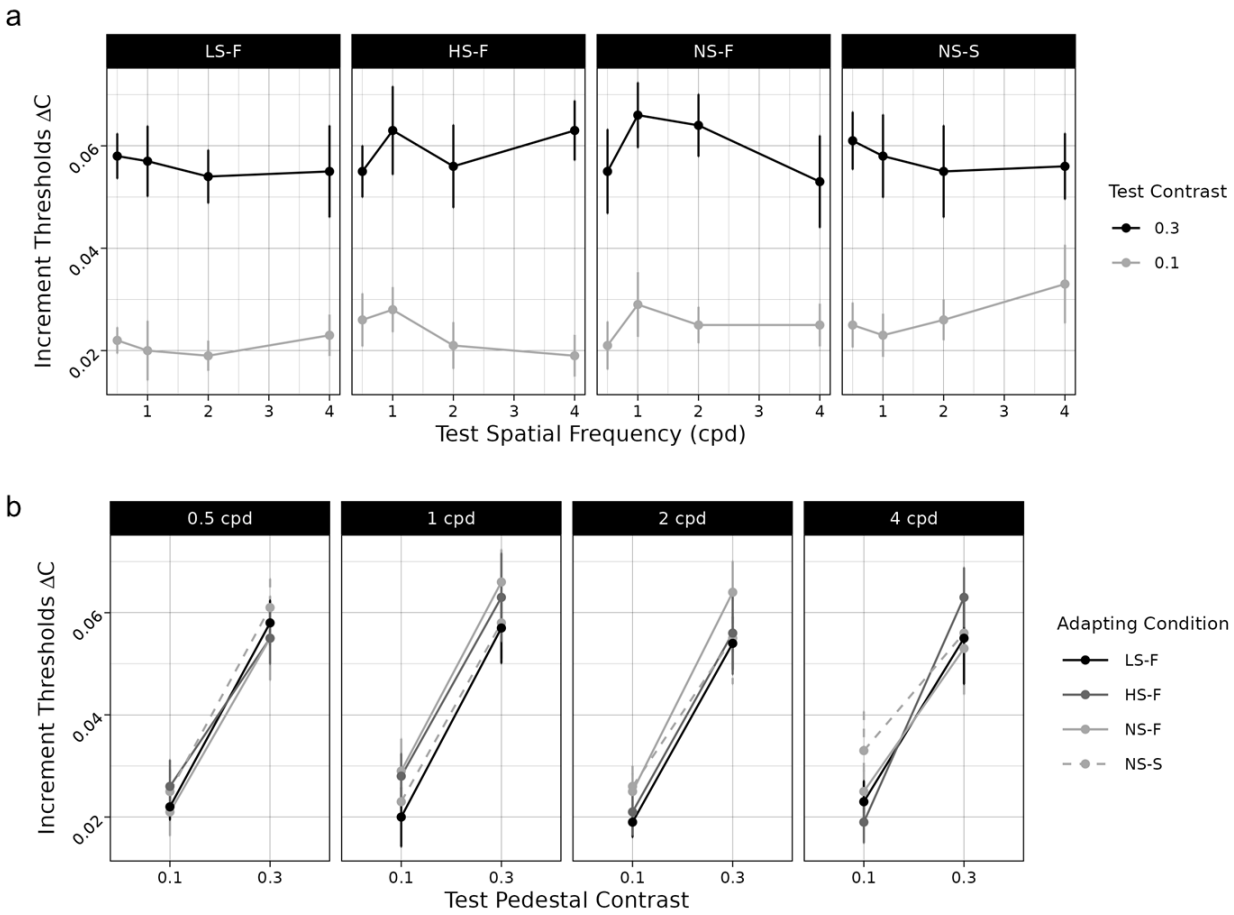

Figure 10. Results of Experiment 2: (a) Increment thresholds (Δ*C*s) for each adapting condition, featuring different spatial frequency components (LS-F: low-spatial frequency filtered flicker, HS-F: high-spatial frequency filtered flicker, NS-F: no-spatial frequency (uniform pattern) flicker, and NS-S: no-spatial frequency (uniform pattern) static adapting condition), plotted against test spatial frequency (cpd). The black line represents the 30% test pedestal contrast condition, and the gray line represents the 10% test pedestal contrast condition. While there is a clear difference in the Δ*C*s between the two pedestal contrast conditions, no significant differences were found among the adapting flicker conditions. (b) Presents the same data as in (a) but formatted differently to facilitate a clearer comparison between the results of Experiments 1 and 2. Here, increment thresholds (Δ*C*s) for various adapting flicker conditions are displayed at four test spatial frequencies, ranging from 0.5 cpd (leftmost panel) to 4 cpd (rightmost panel). Each panel features four lines representing the adapting conditions: LS-F (black solid line), HS-F (dark gray solid line), NS-F (light gray solid line), and NS-S (light gray dashed line).

Figure 11: Results of Experiment 3

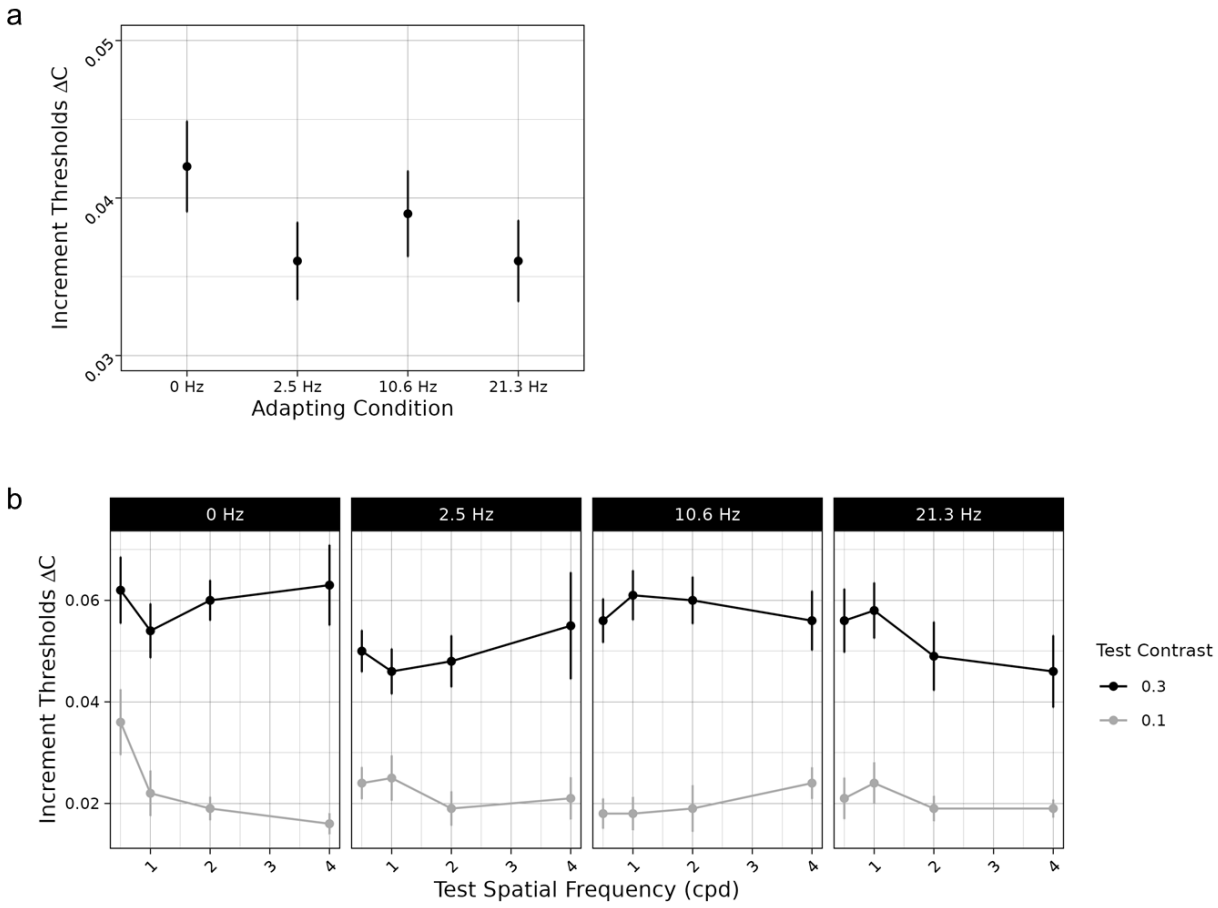

Figure 11. Results of Experiment 3: (a) Increment thresholds (Δ*C*s) plotted against adapting conditions with different temporal frequencies (0 Hz: static adapting condition with a low-pass filtered pattern, 2.5 Hz, 10.6 Hz, and 21.3 Hz). The static 0 Hz condition showed significant differences compared to the other flicker adapting conditions. (b) Displays the same data as in (a) but provides a more detailed analysis. The black line represents the 30% test pedestal contrast condition, while the gray line represents the 10% test pedestal contrast condition. Although there is a clear difference between the ΔCs across the two pedestal contrast conditions, no significant differences were observed among the different adapting flicker conditions.

Figure 12: Further Results of Experiment 3

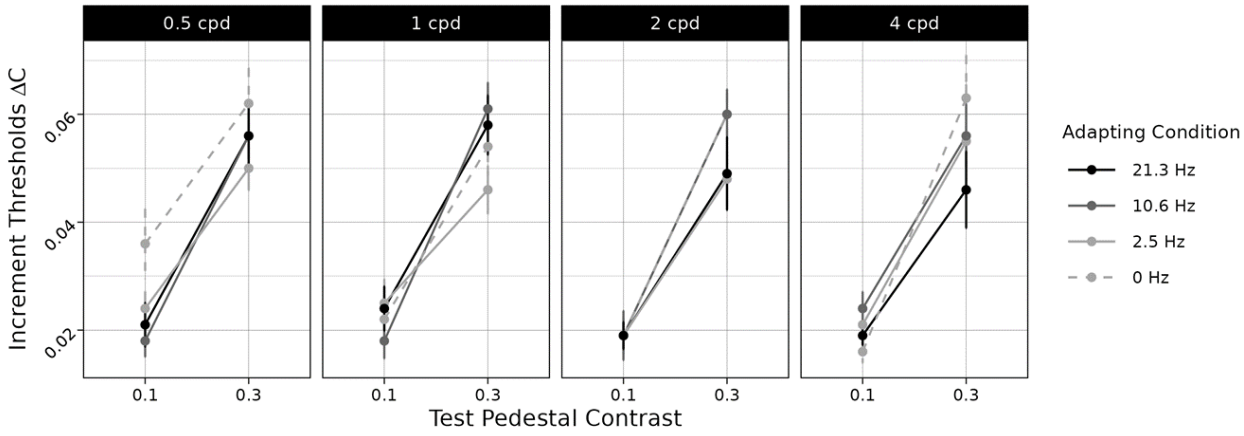

Figure 12. Further results of Experiment 3. This figure displays the same data as in Figure 10b but is organized differently to enable a clearer comparison with the results from Experiments 1 and 2. Here, increment thresholds (ΔCs) for various adapting flicker conditions are shown at four test spatial frequencies, ranging from 0.5 cpd (leftmost panel) to 4 cpd (rightmost panel). Each panel includes four lines representing the different adapting conditions: 21.3 Hz (black solid line), 10.6 Hz (dark gray solid line), 2.5 Hz (light gray solid line), and 0 Hz (static condition, light gray dashed line).

Figure 13: Comparisons of Results of Experiments 2 and 3

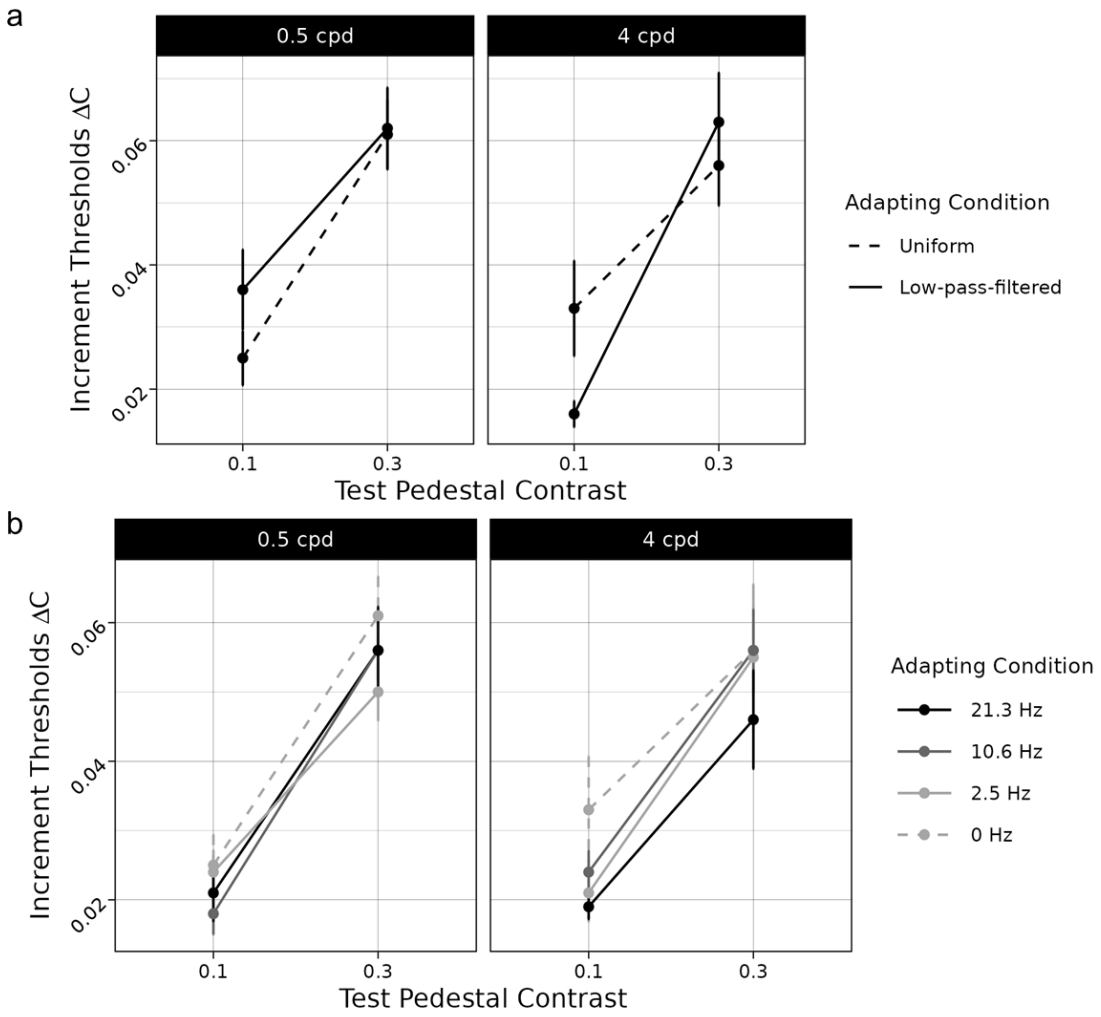

Figure 13. Comparisons of Results of Experiments 2 and 3. (a) Given significant differences in the 0 Hz adapting condition compared to other conditions, we investigated how it differed from the uniform pattern static condition used in Experiment 2. The low-pass filtered pattern at 10% test pedestal contrast for a test spatial frequency of 4 cpd exhibited lower Δ*C*s than the uniform pattern. (b) Further analysis compared the static uniform pattern from Experiment 2 with other adapting conditions from Experiment 3, aiming to align these results with those from earlier experiments. This comparison found no significant differences among the adapting conditions: 21.3 Hz (black solid line), 10.6 Hz (dark gray solid line), 2.5 Hz (light gray solid line), and 0 Hz (static condition, light gray dashed line).

APPENDIX

Much of our understanding of spatial and temporal aspects of human vision comes from research motivated by linear systems theory. For a system to be considered linear, it must adhere to two fundamental principles: homogeneity and additivity. A homogenous system experiences an identical amplitude (intensity) change in the output for a given amplitude change in the input. In other words, if the input's intensity is doubled, the output function will also double. This phenomenon is known as homogeneity or the scalar rule of linear systems. The principle of additivity assumes that the output is the sum of the system's responses to each of the two inputs presented separately, thereby implying homogeneity. The combination of these two principles is referred to as the principle of superposition. Although not all linear systems are shift-invariant, a linear system that is shift-invariant must elicit the same response to inputs at different points in time. The principle of superposition and shift-invariance are highly beneficial as they suggest that, if the human visual system is both linear and shift-invariant, it may be possible to determine the visual system's response to a set of base stimuli at a specific time and use this information to predict the response to any complex stimulus at different points in time. Research has established that the human visual system satisfies not only the principle of superposition but also shift-invariance (for review, see Graham, 1981; Schwartz, 2004).

The characterization of a linear shift-invariant optical system is the Modulation Transfer Function (MTF), i.e., the degree to which information is transferred through the system. Recordings from single cells in the visual system can determine a cell's MTF by measuring its discharge rate for a range of constant-contrast spatial frequencies. However, it is difficult to

determine the transfer characteristic of the entire visual system to various spatial frequencies and contrasts using the same approach. One solution is to use the contrast sensitivity function (CSF), which measures the stimulus amplitude required to produce a constant-response criterion, usually the absolute contrast threshold for pattern detection. Human spatial vision is characterized by the spatial contrast sensitivity function (SCSF), which describes how sensitive an observer is to luminance-defined stimuli of various sizes and contrasts.

A sine wave possesses well-suited properties for measuring shift-invariant linear systems: it is regular and repeating and oscillates around a mean level. It has a zero-value at the origin in both the temporal dimension, at time zero, and in the spatial dimension, at the position of the wave's origin. A single sine wave can be described by three properties: frequency, amplitude, and phase. The distance from one peak of the wave to the next peak is called the wavelength and the number of peaks in the stimulus is frequency. The longer the wavelength, the lower the frequency. In terms of visual angle, spatial frequency can be defined as cycles within a given distance, quantified as cycles per degree (cpd). Sine waves can also have various amplitudes, which represent the difference between the peak (or the trough) and the mean level in the luminance variation. The amplitude of a sine wave is usually perceived as contrast, or the variations between light and dark areas. The location of the wave in space is referred to as phase. There are two types of phase: 1) absolute phase refers to the location of the image components in the visual field, and 2) relative phase refers the location of the components relative to each other. Phase is measured as a fraction of a cycle of 360 degrees since each component consists of repeating cycles. A cosine wave is a phase-shifted version of the sine wave, which differs by a 90 degrees phase angle. It has a value of one at time zero.

The properties of sine waves allow for the decomposition of any stimulus into a series of sine waves at different frequencies that are shifted and scaled. In other words, complex stimuli can be expressed as a combination of component sine waves. For instance, when two identical sine waves are in phase, they lead to constructive interference, which results in a wave with an amplitude equal to the sum of the amplitudes of the two waves. Conversely, when the two sine waves are 180 degrees out of phase, the process of destructive interference or phase cancellation occurs, where the waves cancel each other out, resulting in no wave. When the two waves are in a state between complete phase coherence and complete phase cancellation, they interfere constructively at some points and destructively in others, leading to a sine curve with the same frequency as the two interfering waves. The amplitude of the resulting wave is somewhere between the sum of the amplitudes of the two waves that created it and their difference.

The process of linear system (or Fourier) analysis can be applied to luminance profiles that are spatially aligned to create sinusoidal grating stimuli. These gratings can vary in spatial frequency, orientation, phase, and contrast (amplitude), and have been commonly utilized as fundamental stimuli in research with systematically varied attributes to predict the response of the visual system to more complex stimuli, such as natural scenes. If the visual system were a linear system, then one could predict the detectability of any one-dimensional pattern that varies along a single axis by knowing the observer's sensitivity to sinusoidal gratings of different spatial frequencies. This is why sinusoidal gratings are used as visual stimuli, as they allow for precise and quantitative predictions using a linear systems approach.

The contrast detection experiment is commonly used to measure the SCSF by determining the minimum contrast needed to detect sine wave gratings of varying spatial

frequencies. The sensitivity curve, representing the reciprocal of the threshold function, indicates high sensitivity with low threshold values. The typical human contrast sensitivity function exhibits a band-pass characteristic, with the peak sensitivity occurring at approximately 4 cycles per degree (cpd), an intermediate spatial frequency. The sensitivity decreases on both sides of this peak (Campbell & Robson, 1968). The upper limit of spatial frequency sensitivity, or high-frequency cutoff, of an observer determines their spatial acuity, which refers to the finest spatial patterns they can perceive. In young, healthy adults, the high-frequency cutoff can be around 60 cpd, but this ability generally declines with age.

The SCSF is not believed to be comprised of a single channel that maximally responds to around 4 cpd. Instead, the SCSF is hypothesized to be an envelope that encompasses multiple, narrower channels, potentially independent, each corresponding to a distinct set of neurons with varying preferred spatial frequencies. This multi-channel model of spatial vision is supported by prior adaptation experiments to a particular spatial frequency sine wave grating (Blakemore & Campbell, 1969; Campbell & Robson, 1968), which demonstrated a discrete reduction in sensitivity for gratings with spatial frequencies near that of the adapting grating, but not all frequencies.

Another experiment, using a square wave composed of an infinite sum of odd harmonics, further supports the notion that human spatial vision functions as a linear system. In linear systems analysis, the fundamental frequency of a complex periodic waveform represents the lowest frequency component, with all higher frequency components classified as harmonics of the fundamental. To create a reasonable approximation of a square wave, at least the fundamental and third harmonics need to be included. Blakemore and Campbell (1969) conducted an adaptation experiment using a square wave grating instead of a sine wave grating.

The researchers found a reduction in sensitivity at the fundamental frequency of the square wave, which indicated adaptation to that frequency. In addition, they observed a secondary reduction in sensitivity at the third harmonic frequency, indicating adaptation to the third harmonic. This result suggests that the visual system breaks down the square wave into its fundamental and harmonic components.

Empirical evidence from single-unit electrophysiological recordings in the primate visual cortex supports the idea that the visual system may function as a linear system. Specifically, neurons in the striate cortex have been found to exhibit a high degree of selectivity for particular spatial frequencies (De Valois et al., 1982). This observation suggests that a population of such neurons could provide the physiological foundation for the spatial frequency channels that have been previously discussed.

One of the benefits of adopting a linear systems approach is the existence of extensively developed and easily comprehensible mathematical tools, which allow the formulation of quantitative predictions and the rigorous examination of hypotheses. When a system is linear, its response to any complex input can be predicted based on its response to a single input amplitude for each frequency. However, it's important to note that mathematical techniques such as linear systems analysis are useful when certain conditions are met. This approach assumes that the system being studied is linear, but the visual system's non-linearities, including at threshold (e.g., Green & Swets, 1966), the saturating intensity-response functions of cortical cells (e.g. Brown et al., 2018; Cannon, 1979), and the inhibitory interactions among spatial frequency channels (e.g., De Valois, 1977; Stecher et al., 1973; Tolhurst, 1972), suggest that spatial frequency channels are not entirely independent but may be mutually inhibitory.

Tolhurst's (1972) adaptation experiment provided the first evidence of inhibitory

interactions between spatial frequency channels. He compared the reduction in contrast sensitivity resulting from adapting to a sinusoidal grating and a square wave grating, with the same amplitudes of their fundamentals, *f*. If the channels were independent, both conditions should have produced identical sensitivity reductions at *f*. However, adaptation to the square wave grating led to a smaller reduction in contrast sensitivity in comparison to that observed with the sine wave, suggesting that the channels responsive to *f* and to 3*f* (and/or 5*f*) in the square wave are mutually inhibitory. Tolhurst explained that for the square wave grating, the channel responsive to 3*f* would be stimulated and hence inhibit the channel responsive to *f*, leading to a decrease in overall excitation in the channel centered at *f*. These findings were soon supported by Stecher et al. (1973) who found the lessened adaptational effect of an adapting grating with the addition of a second spatial frequency, even for non-harmonic spatial frequency combinations. This suggested that Tolhurst's findings were not limited to square wave gratings. Tolhurst's findings raise a question as to how Campbell and Robson (1968) observed an exact correspondence between contrast sensitivity and fundamental amplitude for sine and square wave gratings. The difference in the results may be due to the use of suprathreshold patterns by Tolhurst and absolute detection by Campbell and Robson. Threshold contrasts can result in the absence of significant inhibitory influence from subthreshold harmonics. Channel interactions may only occur when each component exceeds its own threshold. Low-contrast patterns may provide evidence of channel independence, but strong conclusions cannot be drawn without considering suprathreshold contrasts.

De Valois (1977) conducted an adaptation study and observed a band-limited reduction in contrast sensitivity centered on the adaptation frequency, consistent with the findings of Blakemore and Campbell (1969). However, De Valois also discovered an increase in contrast

sensitivity to spatial frequencies located two or three octaves away from the adaptation frequency, which suggests that spatial frequency channels inhibit one another. The adaptation of one channel results in a temporary decrease in its activity, reducing the suppression it exerts on other channels, leading to an increase in contrast sensitivity. This finding provides evidence for inter-channel inhibition, which is further supported by De Valois and Switkes (1980).

The research conducted by De Valois and Tootell (1983) offered physiological evidence for spatial frequency interactions. They studied the response of striate cortex cells to patterns of two spatial frequencies and found that nearly all simple cells examined in their study showed a reduction in response to their optimal grating stimulus when presented with other gratings of different harmonically related frequencies. The addition of 2*f* or 3*f* maximally inhibited most cells, with few cells being significantly inhibited by lower spatial frequencies. In comparison, complex cells were less likely to show inhibitory interactions, with only 29% being inhibited by higher spatial frequencies and 8% by lower frequencies. A typical simple cell is unaffected by lower frequency gratings but is inhibited by the addition of either a 2*f* or a 3*f* grating. The findings suggest the possibility of a feedback mechanism, with complex cells tuned to 2*f* or 3*f* providing a major input onto simple cells. This is contrary to the traditional feedforward model where only simple cells transmit information to complex cells without feedback.

It is important to note that although the visual system exhibits a high degree of nonlinearity, within a limited range of intensity, it only displays minor deviations from linearity. Thus, the linear system analysis approach retains its value for analyzing points within this restricted intensity range where the system behaves as a quasi-linear system, particularly in circumstances where low-level mechanisms come into play.

The typical clinical acuity measurement tests the high spatial frequency cutoff. The

Snellen chart, the most widely used clinical acuity test, consists of rows of optotypes (letters) that decrease in size and increase in high spatial frequency content (Schwartz, 2004). The optotypes are typically presented at 100% contrast (black optotypes on a white background) at a constant viewing distance. A patient's acuity level is determined by the size of the smallest optotype they can resolve at a fixed distance. For example, a patient with 20/40 Snellen acuity can resolve at 20 feet what a typical observer can resolve at 40 feet. At the 20/20 acuity level, the optotype subtends 1' arc at 40 feet. If the patient with 20/40 acuity can just barely resolve a grating with bars or gaps subtending 2' arc, then the just-resolvable grating subtends 4' arc. By converting arc minutes to cycles per degree, the patient's high-frequency SCSF cutoff can be determined. For example, a Snellen acuity of 20/40 corresponds to a high-frequency CSF cutoff of 15 cycles per degree, while a Snellen acuity of 20/20 corresponds to a cutoff frequency of 30 cycles per degree.

The use of the Snellen chart to measure visual acuity has limitations. Firstly, each line on the chart has a different number of characters, and the optotypes are not evenly spaced, leading to crowding effects that can reduce acuity, particularly in disorders of central vision, such as amblyopia. Secondly, not all optotypes on the chart are equally discriminable, with some optotypes being easier to discriminate than others. Thirdly, the Snellen chart only tests the ability to resolve optotypes at 100% contrast, which is not representative of the lower contrast stimuli encountered in the visual world. Therefore, while Snellen acuity is a commonly used measure of spatial vision, it only assesses a limited aspect of visual function.

Bailey and Lovie (1976) developed a new eye chart to address the limitations of the Snellen chart. The Bailey-Lovie eye chart overcomes these limitations by presenting each line with the same number of optotypes that are equally legible and with constant relative spacing. A

variation on this idea is the Pelli-Robson approach, which measures threshold contrast using optotypes (Pelli et al., 1988). While determining a SCSF for various contrast levels is impractical for clinical use, the low-contrast visual acuity measured with the Bailey-Lovie and the Pelli-Robson charts are effective tools for identifying reductions in contrast sensitivity. Unlike the Snellen chart, these charts decrease the contrast of optotypes while maintaining their size as the patient reads down the chart, making them efficient alternatives for clinical use.

To briefly touch on common clinical acuity measures, it is noted that these tests focus primarily on the high spatial frequency cut-off point in the CSF. This is accomplished by reducing the size of a feature until it can no longer be resolved, which shifts the pattern's spatial frequency spectrum towards higher frequencies. As a result, acuity tests essentially measure the highest spatial frequencies that can be distinguished at a given contrast level, with a typical maximum of 100%. SCSF, however, measures the lowest contrast detectable at a given spatial frequency. While classical visual acuity measures and SCSF assessments measure different aspects of spatial vision, at the highest spatial frequencies, it is highly probable that they both measure the same characteristic—the high spatial frequency cutoff. This is due to the threshold contrast at the least detectable spatial frequencies approaching 100%.

One of the pivotal capabilities of the visual system is its sensitivity to changes in luminance across temporal frequencies. The temporal dimension of human vision is typified by the Temporal Contrast Sensitivity Function (TCSF), while the SCSF characterizes spatial vision. The TCSF measures the sensitivity of the visual system, usually to a large, spatially uniform field undergoing temporal modulation, or flickering, at a specific frequency. Stimuli at lower temporal frequencies manifest as a slower flicker, while those at higher temporal frequencies present as a faster flicker. In parallel to the SCSF, the TCSF plots sensitivity against temporal

frequency. Analogous to how any spatial stimulus can be synthesized from a combination of spatial sine waves, temporal stimuli can also be generated from a composite of temporal sine waves.

In contrast to the SCSF, which expresses sensitivity in terms of spatial contrast, the TCSF represents sensitivity as the percentage modulation required for a given set of stimulus conditions, such as mean luminance and spatial frequency. A reduced sensitivity to a particular temporal frequency necessitates a higher contrast (i.e., percentage modulation) for stimulus perception. A stimulus with a temporal frequency of 0 Hz appears static, while stimuli with higher frequencies are perceived as flickering. A typical human TCSF peaks at 8−12 Hz (Cass & Alais, 2006; Kelly, 1966; Schwartz, 2004; Wooten et al., 2010). As the temporal frequency increases, the flicker appears to speed up until a threshold is attained where the flickering effect becomes indistinguishable, yielding the perception of a steady image. This threshold is often referred to as the critical flicker fusion frequency (CFF). The CFF generally falls within the range of 50 to 60 Hz (de Lange Dzn, 1958; Kelly, 1961, 1972; Kulikowski & Tolhurst, 1973; Lloyd & Landis, 1960; Regan, 1968). Furthermore, it has been observed that the CFF increases logarithmically in relation to the stimulus area (e.g., Granit & Harper, 1930).

As previously discussed, inhibitory interactions are evident in spatial frequency channels. Likewise, temporal frequency channels also exhibit inhibitory interactions, as demonstrated by Cass and Alais (2006), who observed that the high temporal frequency channel is capable of suppressing the low temporal frequency channel, suggesting that suppressing the high channel could increase activity in the low channel.

The TCSF has been measured in human observers using various spatial and temporal configurations. The first TCSFs obtained by de Lange Dzn (1954, 1958) at different luminance

levels showed low-pass filtering properties, suggesting that the human visual system behaves as a linear system. Specifically, de Lange found that sensitivity was relatively consistent for temporal frequencies below 10 Hz, but declined rapidly for frequencies above 10 Hz. He suggested that if the temporal filter were band-pass, the TCSF would have peak sensitivity at moderate frequencies with decreasing sensitivity in both high and low frequency directions.

Kelly (1959) later proposed that the low-pass filtering observed in the TCSF obtained by de Lange Dzn (1954, 1958) was due to fast eye movements across sharp edges in the stimulus at low temporal frequencies. To test this hypothesis, Kelly conducted experiments using two test fields, one with a blurred edge and the other with a dark surround to reduce the effects of eye movements. The TCSFs obtained under these conditions showed sharply band-pass filtering behavior. However, this eye movement hypothesis was later contested by a series of studies that stabilized the retinal image (Keesey, 1970, 1972; Kelly, 1983, 1984), as discussed later.

Using sine wave gratings, Robson (1966) identified distinct patterns of sensitivity. Temporal sensitivity displayed a low-pass pattern at high spatial frequencies and a band-pass pattern at low spatial frequencies, while spatial sensitivity showed a low-pass pattern at high temporal frequencies and a band-pass pattern at low temporal frequencies. Specifically, for 4, 16, and 22 cpd gratings, the TCSFs were all low-pass, with peak sensitivity at 0.5 Hz, the lowest temporal frequency tested. General sensitivity increased as spatial frequency decreased from 22 to 4 cpd. However, for 0.5 cpd gratings, the TCSF was band-pass, with peak sensitivity around 5 Hz and decreasing sensitivity on both sides of the peak. Above 5 Hz, the TCSF curves for 0.5 and 4 cpd gratings coincided, but the 4 cpd curve was low-pass. The SCSFs for 6, 16, and 22 Hz were all low-pass, peaking at the lowest tested spatial frequency of 0.5 cpd. Similar to TCSFs, there was an overall increase in sensitivity as temporal frequency decreased. However, the SCSF

for 1 Hz was band-pass, with peak sensitivity at 4 cpd, and sensitivities above 3 cpd were similar to those for 6 Hz modulation.

Van Nes et al. (1967) reported comparable findings, using drifting rather than flickering sine wave gratings. Although the threshold for perception of a moving grating is generally higher than that for detection of flicker, TCSFs obtained by Van Nes et al. were similar to those of Robson (1966). For spatial frequencies greater than 0.64 cpd, the TCSFs were low-pass, but the curve was band-pass for 0.64 cpd, which was the lowest spatial frequency investigated. Sensitivities for all spatial frequencies decreased with temporal frequencies greater than 1-2 Hz. The SCSFs for temporal frequencies of 0 and 1 Hz were band-pass, as Robson had found. However, their findings were inconsistent with Robson's for high temporal frequencies. The SCSF for 10 Hz of van Nes et al. was band-pass, while Robson's SCSFs for 6, 16, and 22 Hz were all low-pass.

These studies aimed to systematically measure spatiotemporal contrast sensitivity functions with less precise control over temporal frequency compared to modern stabilization techniques. However, Keesey (1970) reported no significant differences between unstabilized and stabilized viewing for 0.5°, 1°, and 2° fields in dark surrounds. For a 1° field in an equiluminant surround, a sensitivity decrease to flicker resulted from retinal image stabilization. Keesey (1972) also observed reduced sensitivity for a flickering vertical bar (1° in length and 4' of arc in width) in an equiluminant surround. Comparing two categories of judgments, flicker detection and pattern detection, the TCSF for flicker detection showed a band-pass profile with peak sensitivity around 8 Hz, while the TCSF for pattern detection exhibited a low-pass pattern with decreasing sensitivity above 3 Hz.

Kulikowski and Tolhurst (1973) expanded on the previous works of van Nes et al. (1967)

and Keesey (1972) by examining flicker detection thresholds and pattern detection thresholds at various spatial and temporal frequencies under unstabilized viewing conditions. The SCSFs for flicker detection at both 3.5 Hz and 8 Hz were found to be low-pass. In contrast, the SCSFs for pattern detection at 3.5 Hz were band-pass with a peak of approximately 5 cpd, while those at 8 Hz were flattened over the entire range of spatial frequency. The TCSFs obtained in their study were consistent with the findings of Robson and Kelly for low (0.8 cpd) and high (12 cpd) spatial frequencies, as well as those of Keesey (1972) for flicker and pattern criteria. The TCSFs for flicker detection were band-pass, peaking at approximately 5 Hz, while the TCSFs for pattern detection were low-pass. The shape of the two types of TCSF remained consistent irrespective of the spatial frequency. A change in the frequency of the grating produced a shift in overall sensitivity, without affecting the TCSF's shape. These findings suggest that the TCSF behaves like a linear system that is shift-invariant.

Kulikowski and Tolhurst (1973) also found that the perception of a flickering grating was dependent on the conditions that produced either higher flicker or pattern sensitivity. Specifically, under higher flicker sensitivity, the grating was perceived as a uniform flickering field near the threshold, while under higher pattern sensitivity, it was perceived as a static grating near the threshold. They interpreted these results as evidence for two distinct visual mechanisms, one for form processing and one for motion processing, which aligns with now the established role of the P and M pathways in visual processing.

Complementing the findings of Kulikowski and Tolhurst, Kelly (1983, 1984) used retinal image stabilization and movement to investigate the spatial and temporal frequency channels' response to moving sine-wave gratings. Kelly found a band-pass SCSF when sine-wave gratings were drifted at low temporal frequencies (≤1 Hz). However, as the temporal frequency increased,

sensitivity to high spatial frequencies decreased slightly while sensitivity to low spatial frequencies showed a large increase. At low temporal frequencies, the low spatial frequency attenuation is profound, resulting in a band-pass SCSF, whereas at high temporal frequencies, the SCSF becomes low-pass.

Single-unit electrophysiological recordings in the LGN also support these previous findings (Kaplan, 2004; Kaplan & Shapley, 1984; Kaplan & Shapley, 1982; Kaplan & Shapley, 1986). For instance, Kaplan and Shapley (1982) demonstrated that the cells in the two M layers are ten times more sensitive at low to medium spatial frequencies when medium temporal frequencies are presented.

As previously discussed, the assumption of independence in linear systems has been challenged by the presence of dynamic interplay within a single dimension. Furthermore, behavioral research on topics such as masking (Breitmeyer et al., 1981; Breitmeyer & Ganz, 1976; Breitmeyer & Ganz, 1977; Breitmeyer & Williams, 1990; Hess & Snowden, 1992), figure-ground perception (Brown & Weisstein, 1988; Weisstein & Brannan, 1991; Weisstein et al., 1992), and continuous flash suppression (CFS) (Han et al., 2018; Han et al., 2019; Han et al., 2016), has underscored the intertwined nature of temporal and spatial channels, proposing that this relationship is modulated by the relative activities of the M and P pathways.

REFERENCES

Afraz, S.-R., Kiani, R., & Esteky, H. (2006). Microstimulation of inferotemporal cortex influences face categorization. *Nature*, *442*(7103), 692-695.

Anderson, S. F., Kelley, K., & Maxwell, S. E. (2017). Sample-size planning for more accurate statistical power: a method adjusting sample effect sizes for publication bias and uncertainty. *Psychological Science*, *28*(11), 1547-1562. https://doi.org/10.1177/0956797617723724

Archer, D. R., Alitto, H. J., & Usrey, W. M. (2021). Stimulus contrast affects spatial integration in the lateral geniculate nucleus of macaque monkeys. *Journal of Neuroscience*, *41*(29), 6246-6256.

Arnold, D. H., Williams, J. D., Phipps, N. E., & Goodale, M. A. (2016). Sharpening vision by adapting to flicker. *Proceedings of the National Academy of Sciences of the United States of America*, *113*(44), 12556-12561. https://doi.org/10.1073/pnas.1609330113

Bailey, I. L., & Lovie, J. E. (1976). New design principles for visual acuity letter charts. *Am J Optom Physiol Opt*, *53*(11), 740-745. https://doi.org/10.1097/00006324-197611000-00006

Bartlett, L. K., Graf, E. W., & Adams, W. J. (2018). The effects of attention and adaptation duration on the motion aftereffect. *Journal of Experimental Psychology: Human Perception and Performance*, *44*(11), 1805.

Blakemore, C., & Campbell, F. W. (1969). On existence of neurones in human visual system selectively sensitive to orientation and size of retinal images. *Journal of Physiology-London*, *203*(1), 237-260. https://doi.org/10.1113/jphysiol.1969.sp008862

Breitmeyer, B., & Julesz, B. (1975). Role of on and Off Transients in Determining Psychophysical Spatial Frequency-Response. *Vision Research*, *15*(3), 411-415. https://doi.org/10.1016/0042-6989(75)90090-5

Breitmeyer, B., Levi, D. M., & Harwerth, R. S. (1981). Flicker Masking in Spatial Vision. *Vision Research*, *21*(9), 1377-1385. https://doi.org/10.1016/0042-6989(81)90243-1

Breitmeyer, B. G. (1973). A relationship between the detection of size, rate, orientation and direction in the human visual system. *Vision Research*, *13*(1), 41-58.

Breitmeyer, B. G. (2007). Visual masking: past accomplishments, present status, future developments. *Advances in cognitive psychology*, *3*(1-2), 9. https://doi.org/10.2478/v10053-008-0010-7

Breitmeyer, B. G., & Ganz, L. (1976). Implications of sustained and transient channels for theories of visual-pattern masking, saccadic suppression, and information-processing. *Psychological Review*, *83*(1), 1-36. https://doi.org/10.1037/0033-295x.83.1.1

Breitmeyer, B. G., & Ganz, L. (1977). Temporal studies with flashed gratings: Inferences about human transient and sustained channels. *Vision Research*, *17*(7), 861-865.

Breitmeyer, B. G., & Öğmen, H. (2006). *Visual masking: Time slices through conscious and unconscious vision*. Oxford University Press.

Breitmeyer, B. G., & Williams, M. C. (1990). Effects of isoluminant-background color on metacontrast and stroboscopic motion: Interactions between sustained (P) and transient (M) channels. *Vision Research*, *30*(7), 1069-1075.

Brown, J. M. (2018). *Pioneer visual neuroscience: a festschrift for Naomi Weisstein*. Routledge.

Brown, J. M., Breitmeyer, B. G., Hale, R. G., & Plummer, R. W. (2018). Contrast Sensitivity Indicates Processing Level of Visual Illusions. *Journal of Experimental Psychology-Human Perception and Performance*, *44*(10), 1557-1566. https://doi.org/10.1037/xhp0000554

Brown, J. M., & Weisstein, N. (1988). A spatial frequency effect on perceived depth. *Perception & Psychophysics*, *44*(2), 157-166. https://doi.org/10.3758/BF03208708

Burr, D. (2011). Visual perception: More than meets the eye. *Current Biology*, *21*(4), R159-R161.

Campbell, F. W., & Robson, J. G. (1968). Application of Fourier analysis to the visibility of gratings. *J Physiol*, *197*(3), 551-566. https://doi.org/10.1113/jphysiol.1968.sp008574

Cannon, M. W. (1979). Contrast sensation: a linear function of stimulus contrast. *Vision Research*, *19*(9), 1045-1052.

Cass, J., & Alais, D. (2006). Evidence for two interacting temporal channels in human visual processing. *Vision Research*, *46*(18), 2859-2868. https://doi.org/10.1016/j.visres.2006.02.015

Choi, L. K., Bovik, A. C., & Cormack, L. K. (2016). The effect of eccentricity and spatiotemporal energy on motion silencing. *Journal of Vision*, *16*(5), 19. https://doi.org/10.1167/16.5.19

de Lange Dzn, H. (1954). Relationship between Critical Flicker-Frequency and a Set of Low-Frequency Characteristics of the Eye. *Journal of the Optical Society of America*, *44*(5), 380-389. https://doi.org/10.1364/Josa.44.000380

de Lange Dzn, H. (1958). Research into the dynamic nature of the human fovea-cortex systems with intermittent and modulated light. I. Attenuation characteristics with white and colored light. *Journal of the Optical Society of America*, *48*(11), 777-784. https://doi.org/10.1364/Josa.48.000777

De Valois, K. K. (1977). Spatial frequency adaptation can enhance contrast sensitivity. *Vision Research*, *17*(9), 1057-1065.

De Valois, K. K., & Switkes, E. (1980). Spatial frequency specific interaction of dot patterns and gratings. *Proceedings of the National Academy of Sciences*, *77*(1), 662-665.

De Valois, K. K., & Tootell, R. B. (1983). Spatial-frequency-specific inhibition in cat striate cortex cells. *The Journal of physiology*, *336*(1), 359-376.

De Valois, R. L., Albrecht, D. G., & Thorell, L. G. (1982). Spatial frequency selectivity of cells in macaque visual cortex. *Vision Research*, *22*(5), 545-559.

Derrington, A. M., & Lennie, P. (1984). Spatial and temporal contrast sensitivities of neurones in lateral geniculate nucleus of macaque. *The Journal of physiology*, *357*(1), 219-240. https://doi.org/10.1113/jphysiol.1984.sp015498

Erlikhman, G., Gutentag, S., Blair, C. D., & Caplovitz, G. P. (2019). Interactions of flicker and motion. *Vision Research*, *155*, 24-34. https://doi.org/https://doi.org/10.1016/j.visres.2018.12.005

Faivre, N., & Koch, C. (2014). Temporal structure coding with and without awareness. *Cognition*, *131*(3), 404-414.

Graham, N. (1981). The visual system does a crude Fourier analysis of patterns. *Mathematical psychology and psychophysiology*, 1-16.

Granit, R., & Harper, P. (1930). Comparative studies on the peripheral and central retina: II. Synaptic reactions in the eye. *American Journal of Physiology-Legacy Content*, *95*(1), 211-228.

Green, D. M., & Swets, J. A. (1966). *Signal detection theory and psychophysics* (Vol. 1). Wiley New York.

Han, S., Blake, R., & Alais, D. (2018). Slow and steady, not fast and furious: Slow temporal modulation strengthens continuous flash suppression. *Consciousness and Cognition*, *58*, 10-19. https://doi.org/10.1016/j.concog.2017.12.007

Han, S., Lukaszewski, R., & Alais, D. (2019). Continuous flash suppression operates in local spatial zones: Effects of mask size and contrast. *Vision Research*, *154*, 105-114.

Han, S., Lunghi, C., & Alais, D. (2016). The temporal frequency tuning of continuous flash suppression reveals peak suppression at very low frequencies. *Scientific Reports*, *6*. https://doi.org/10.1038/srep35723

Hess, R. F., & Snowden, R. J. (1992). Temporal Properties of Human Visual Filters - Number, Shapes and Spatial Covariation. *Vision Research*, *32*(1), 47-59. https://doi.org/10.1016/0042-6989(92)90112-V

Hicks, T. P., Lee, B. B., & Vidyasagar, T. R. (1983). The responses of cells in macaque lateral geniculate nucleus to sinusoidal gratings. *The Journal of physiology*, *337*(1), 183-200. https://doi.org/https://doi.org/10.1113/jphysiol.1983.sp014619

Huk, A. C., Ress, D., & Heeger, D. J. (2001). Neuronal basis of the motion aftereffect reconsidered. *Neuron*, *32*(1), 161-172. https://doi.org/10.1016/s0896-6273(01)00452-4

Kandel, E. R., Schwartz, J. H., Jessell, T. M., Siegelbaum, S., Hudspeth, A. J., & Mack, S. (2000). *Principles of neural science* (Vol. 4). McGraw-hill New York.

Kaneko, S., Giaschi, D., & Anstis, S. (2015). Flicker adaptation or superimposition raises the apparent spatial frequency of coarse test gratings. *Vision Research*, *108*, 85-92. https://doi.org/10.1016/j.visres.2015.01.005

Kaplan, E. (2004). The M, P and K pathways of the primate visual system. In J. S. Werner & L. M. Chalupa (Eds.), *The visual neurosciences* (Vol. 46). Mit Press.

Kaplan, E., Purpura, K., & Shapley, R. M. (1987). Contrast affects the transmission of visual information through the mammalian lateral geniculate nucleus. *The Journal of physiology*, *391*(1), 267-288.

Kaplan, E., & Shapley, R. (1984). The origin of the S (slow) potential in the mammalian lateral geniculate nucleus. *Experimental Brain Research*, *55*(1), 111-116.

Kaplan, E., & Shapley, R. M. (1982). X and Y cells in the lateral geniculate nucleus of macaque monkeys. *The Journal of physiology*, *330*(1), 125-143.

Kaplan, E., & Shapley, R. M. (1986). The primate retina contains two types of ganglion-cells, with high and low contrast sensitivity. *Proceedings of the National Academy of Sciences of the United States of America*, *83*(8), 2755-2757. https://doi.org/10.1073/pnas.83.8.2755

Kaunitz, L. N., Fracasso, A., Skujevskis, M., & Melcher, D. (2014). Waves of visibility: probing the depth of inter-ocular suppression with transient and sustained targets. *Frontiers in Psychology*, *5*, 804.

Keesey, U. T. (1970). Variables determining flicker sensitivity in small fields. *Journal of the Optical Society of America*, *60*(3), 390-398. https://doi.org/10.1364/Josa.60.000390

Keesey, U. T. (1972). Flicker and pattern detection: a comparison of thresholds. *Journal of the Optical Society of America*, *62*(3), 446-448. https://doi.org/10.1364/Josa.62.000446

Kelly, D. H. (1959). Effects of sharp edges in a flickering field. *Journal of the Optical Society of America*, *49*(7), 730-732. https://doi.org/10.1364/Josa.49.000730

Kelly, D. H. (1961). Visual responses to time-dependent stimuli. 1. amplitude sensitivity measurements. *Journal of the Optical Society of America*, *51*(4), 422-429. https://doi.org/10.1364/Josa.51.000422

Kelly, D. H. (1966). Frequency doubling in visual responses. *JOSA*, *56*(11), 1628-1633.

Kelly, D. H. (1972). Adaptation effects on spatio-temporal sine-wave thresholds. *Vision Research*, *12*(1), 89-101. https://doi.org/10.1016/0042-6989(72)90139-3

Kelly, D. H. (1983). Spatiotemporal Variation of Chromatic and Achromatic Contrast Thresholds. *Journal of the Optical Society of America*, *73*(6), 742-750. https://doi.org/10.1364/Josa.73.000742

Kelly, D. H. (1984). Retinal Inhomogeneity .1. Spatiotemporal Contrast Sensitivity. *Journal of the Optical Society of America a-Optics Image Science and Vision*, *1*(1), 107-113. https://doi.org/10.1364/Josaa.1.000107

Klymenko, V., Weisstein, N., Topolski, R., & Hsieh, C. H. (1989). Spatial and temporal frequency in figure-ground organization. *Perception & Psychophysics*, *45*(5), 395-403. https://doi.org/10.3758/BF03210712

Kulikowski, J. J., & Tolhurst, D. J. (1973). Psychophysical evidence for sustained and transient detectors in human vision. *J Physiol*, *232*(1), 149-162. https://doi.org/10.1113/jphysiol.1973.sp010261

Lee, B. B., Pokorny, J., Smith, V. C., Martin, P. R., & Valberg, A. (1990). Luminance and chromatic modulation sensitivity of macaque ganglion cells and human observers.

Journal of the Optical Society of America A, 7(12), 2223-2236. https://doi.org/10.1364/JOSAA.7.002223

Lee, J., & Chong, S. C. (2021). Quality of average representation can be enhanced by refined individual items. *Attention Perception & Psychophysics, 83*(3), 970-981. https://doi.org/10.3758/s13414-020-02139-3

Legge, G. E. (1978). Sustained and transient mechanisms in human vision: temporal and spatial properties. *Vision Research, 18*(1), 69-81. https://doi.org/10.1016/0042-6989(78)90079-2

Leopold, D. A., Bondar, I. V., & Giese, M. A. (2006). Norm-based face encoding by single neurons in the monkey inferotemporal cortex. *Nature, 442*(7102), 572-575.

Lloyd, V. V., & Landis, C. (1960). Role of the light-dark ratio as a determinant of the flicker-fusion threshold. *Journal of the Optical Society of America, 50*(4), 332-336. https://doi.org/10.1364/Josa.50.000332

MacLeod, D. I. A. (1978). Visual Sensitivity. *Annual review of psychology, 29*(Volume 29, 1978), 613-645. https://doi.org/https://doi.org/10.1146/annurev.ps.29.020178.003145

Mantiuk, R. K., Ashraf, M., & Chapiro, A. (2022). stelaCSF - A Unified Model of Contrast Sensitivity as the Function of Spatio-Temporal Frequency, Eccentricity, Luminance and Area. *ACM Transactions on Graphics, 41*(4). https://doi.org/10.1145/3528223.3530115

Merigan, W. H., & Maunsell, J. H. (1993). How parallel are the primate visual pathways? *Annual Review of Neuroscience, 16*(1), 369-402.

Movshon, J. A., & Lennie, P. (1979). Pattern-selective adaptation in visual cortical neurones. *Nature, 278*(5707), 850-852. https://doi.org/10.1038/278850a0

Murd, C., & Bachmann, T. (2011). Spatially localized motion aftereffect disappears faster from awareness when selectively attended to according to its direction. *Vision Research*, *51*(10), 1157-1162. https://doi.org/10.1016/j.visres.2011.03.008

Nishida, S. y., & Ashida, H. (2000). A hierarchical structure of motion system revealed by interocular transfer of flicker motion aftereffects. *Vision Research*, *40*(3), 265-278. https://doi.org/10.1016/S0042-6989(99)00176-5

Peirce, J. W. (2007). PsychoPy--Psychophysics software in Python. *J Neurosci Methods*, *162*(1-2), 8-13. https://doi.org/10.1016/j.jneumeth.2006.11.017

Peirce, J. W. (2013). Is it just motion that silences awareness of other visual changes? *Journal of Vision*, *13*(7), 17-17. https://doi.org/10.1167/13.7.17

Pelli, D. G., Robson, J. G., & Wilkins, A. J. (1988). The Design of a New Letter Chart for Measuring Contrast Sensitivity. *Clinical Vision Sciences*, *2*(3), 187-199.

Pokorny, J., & Smith, V. C. (1997). Psychophysical signatures associated with magnocellular and parvocellular pathway contrast gain. *Journal of the Optical Society of America a-Optics Image Science and Vision*, *14*(9), 2477-2486. https://doi.org/10.1364/Josaa.14.002477

Purpura, K., Kaplan, E., & Shapley, R. M. (1988). Background light and the contrast gain of primate P and M retinal ganglion cells. *Proceedings of the National Academy of Sciences*, *85*(12), 4534-4537. https://doi.org/10.1073/pnas.85.12.4534

Regan, D. (1968). A High Frequency Mechanism Which Underlies Visual Evoked Potentials. *Electroencephalography and Clinical Neurophysiology*, *25*(3), 231-237. https://doi.org/10.1016/0013-4694(68)90020-5

Robson, J. G. (1966). Spatial and Temporal Contrast-Sensitivity Functions of Visual System. *Journal of the Optical Society of America*, *56*(8), 1141-&. https://doi.org/10.1364/Josa.56.001141

Rodola, G. (2020). Psutil documentation. In: Psutil. https://psutil. readthedocs. io/en/latest.

Schwartz, S. H. (2004). *Visual perception: A clinical orientation*. McGraw-Hill Medical Pub. Division.

Sclar, G., Lennie, P., & DePriest, D. D. (1989). Contrast adaptation in striate cortex of macaque. *Vision Research*, *29*(7), 747-755. https://doi.org/https://doi.org/10.1016/0042-6989(89)90087-4

Solomon, S. G., Peirce, J. W., Dhruv, N. T., & Lennie, P. (2004). Profound contrast adaptation early in the visual pathway. *Neuron*, *42*(1), 155-162. https://doi.org/10.1016/S0896-6273(04)00178-3

Song, J., Breitmeyer, B. G., & Brown, J. M. (2024a). Examining Increment thresholds as a function of pedestal contrast under hypothetical parvo- and magnocellular-biased conditions. *Attention, Perception, & Psychophysics*, *86*(1), 213-220. https://doi.org/10.3758/s13414-023-02819-w

Song, J., Breitmeyer, B. G., & Brown, J. M. (2024b). Further Examination of the Pulsed-and Steady-Pedestal Paradigms under Hypothetical Parvocellular-and Magnocellular-Biased Conditions. *Vision*, *8*(2), 28. https://doi.org/10.3390/vision8020028

Stecher, S., Sigel, C., & Lange, R. (1973). Composite adaptation and spatial frequency interactions. *Vision Research*, *13*(12), 2527-2531.

Suchow, J. W., & Alvarez, G. A. (2011). Motion silences awareness of visual change. *Current Biology*, *21*(2), 140-143.

Sugase-Miyamoto, Y., Matsumoto, N., & Kawano, K. (2011). Role of temporal processing stages by inferior temporal neurons in facial recognition. *Frontiers in Psychology*, *2*, 141.

Sun, H., Lee, B. B., & Baraas, R. C. (2008). Systematic misestimation in a vernier task arising from contrast mismatch. *Visual Neuroscience*, *25*(3), 365-370. https://doi.org/10.1017/S0952523808080188

Tolhurst, D. J. (1972). Adaptation to square-wave gratings: inhibition between spatial frequency channels in the human visual system. *The Journal of physiology*, *226*(1), 231-248.

Tolhurst, D. J., & Movshon, J. A. (1975). Spatial and Temporal Contrast Sensitivity of Striate Cortical-Neurons. *Nature*, *257*(5528), 674-675. https://doi.org/10.1038/257674a0

Tootell, R. B., & Nasr, S. (2017). Columnar segregation of magnocellular and parvocellular streams in human extrastriate cortex. *Journal of Neuroscience*, *37*(33), 8014-8032. https://doi.org/10.1523/Jneurosci.0690-17.2017

Tsuchiya, N., Koch, C., Gilroy, L. A., & Blake, R. (2006). Depth of interocular suppression associated with continuous flash suppression, flash suppression, and binocular rivalry. *Journal of Vision*, *6*(10), 6-6.

Turi, M., & Burr, D. (2013). The "motion silencing" illusion results from global motion and crowding. *Journal of Vision*, *13*(5), 14-14.

van de Grind, W. A., van der Smagt, M. J., & Verstraten, F. A. J. (2004). Storage for free: a surprising property of a simple gain-control model of motion aftereffects. *Vision Research*, *44*(19), 2269-2284. https://doi.org/10.1016/j.visres.2004.04.012

Vogels, R. (2022). More than the face: Representations of bodies in the inferior temporal cortex. *Annual review of vision science*, *8*, 383-405.

Watson, A. B., & Ahumada, A. J. (2005). A standard model for foveal detection of spatial contrast. *Journal of Vision*, *5*(9), 6-6.

Watson, A. B., & Pelli, D. G. (1983). Quest - a bayesian adaptive psychometric method. *Perception & Psychophysics*, *33*(2), 113-120. https://doi.org/10.3758/Bf03202828

Wehrhahn, C., & Westheimer, G. (1990). How vernier acuity depends on contrast. *Experimental Brain Research*, *80*, 618-620.

Weisstein, N., & Brannan, J. R. (1991). A low spatial frequency, red sine wave grating will float in front of gratings with the same or similar spatial frequency but other chromaticities: M and P interactions in figure-ground perception. Investigative ophthalmology & visual science, Sarasota, Florida.

Weisstein, N., Maguire, W., & Brannan, J. R. (1992). M and P pathways and the perception of figure and ground. In J. R. Brannan (Ed.), *Advances in psychology: Applications of parallel processing in vision* (Vol. 86, pp. 137-166). Elsevier BV.

Wooten, B. R., Renzi, L. M., Moore, R., & Hammond, B. R. (2010). A practical method of measuring the human temporal contrast sensitivity function. *Biomedical optics express*, *1*(1), 47-58.

Yamane, S., Kaji, S., & Kawano, K. (1988). What facial features activate face neurons in the inferotemporal cortex of the monkey? *Experimental Brain Research*, *73*, 209-214.

Ye, J., Sinha, P. W., Hou, F., He, X. H., Shen, M. X., Lu, F., & Shao, Y. L. (2021). Impact of Temporal Visual Flicker on Spatial Contrast Sensitivity in Myopia. *Frontiers in Neuroscience*, *15*. https://doi.org/10.3389/fnins.2021.710344